RESEARCH

ELSEVIER

Ionic conductive polymers as artificial solid electrolyte interphase films in Li metal batteries – A review

Shilun Gao [1], Feiyuan Sun [1], Nian Liu [2], Huabin Yang [1,3,*], Peng-Fei Cao [4,*]

[1] Institute of New Energy Material Chemistry, School of Materials Science and Engineering, Nankai University, Tianjin 300350, China
[2] School of Chemical and Biomolecular Engineering, Georgia Institute of Technology, Atlanta, GA 30332, USA
[3] Tianjin Key Laboratory of Metal and Molecule Based Material Chemistry, School of Materials Science and Engineering, Nankai University, Tianjin 300350, China
[4] Chemical Sciences Division, Oak Ridge National Laboratory, Oak Ridge, TN 37830, USA

Lithium (Li) metal has been considered as the ultimate anode material for next-generation recharge-able batteries due to its ultra-high theoretical specific capacity (3860 mAh g^{-1}) and the lowest reduction voltage (-3.04 V vs the standard hydrogen electrode). However, the dendritic Li formation, uncontrolled interfacial reactions, and huge volume variations lead to unstable solid electrolyte interphase (SEI) layer, low Coulombic efficiency and hence short cycling lifetime. Designing artificial solid electrolyte interphase (artificial SEI) films on the Li metal electrode exhibits great potential to solve the aforementioned problems and enable Li–metal batteries with prolonged lifetime. Polymer materials with good ionic conductivity, superior processability and high flexibility are considered as ideal artificial SEI film materials. In this review, according to the ionic conductive groups, recent advances in polymeric artificial SEI films are summarized to afford a deep understanding of Li ion plating/stripping behavior and present design principles of high-performance artificial SEI films in achieving stable Li metal electrodes. Perspectives regarding to the future research directions of polymeric artificial SEI films for Li–metal electrode are also discussed. The insights and design principles of polymeric artificial SEI films gained in the current review will be definitely useful in achieving the Li–metal batteries with improved energy density, high safety and long cycling lifetime toward next-generation energy storage devices.

Keywords: Artificial solid electrolyte interphase; Polymer materials; Ionic conducting; Li metal batteries

Introduction

With the ever-increasing demand of portable electronics, electric vehicles and grid-scale storage, rechargeable batteries with high energy density are highly desired [1–6]. The energy density of rechargeable batteries is related with different parameters, and the specific capacities and operating voltages of cathodes and anodes are the key parameters in determining their ultimate values [7,8]. The cell level energy densities of current commercial lithium-ion batteries (LIBs) are ~240 Wh kg^{-1} or ~640 Wh L^{-1} based on the total weight or volume, respectively [9,10]. With specific capacity and delithiation voltage of the commercial graphite anode being 372 mAh g^{-1} and 0–0.2 V, respectively, anode materials with high specific capacity and low lithiation/delithiation voltage are always preferred [11–15]. Lithium (Li) metal having ultra-high theoretical specific capacity (3860 mAh g^{-1}) and lowest reduction voltage (-3.04 V vs the standard hydrogen electrode) has been considered as the "Holy Grail" anode material in advanced rechargeable batteries [16–22]. Generally speaking, Li metal batteries (LMBs) refer to the rechargeable batteries with

* Corresponding authors.
  E-mail addresses: Yang, H. (hb_yang@nankai.edu.cn), Cao, P.-F. (caop@ornl.gov).

RESEARCH

Li metal as anode, and based on the types of cathode materials, LMBs can be divided into several categories, such as Li–sulfur (Li–S) batteries, Li–air (Li–O_2) batteries and Li–lithium metallic oxide (Li–LMO) batteries [23]. The ultrahigh theoretical energy densities of the LMBs ($\sim$3500 Wh kg^{-1} in Li–O_2 battery, $\sim$2600 Wh kg^{-1} in Li–S battery and $1000 \sim 1500$ Wh kg^{-1} in Li–LMO battery) make them highly promising for next-generation energy storage systems [24–27].

However, LMBs have been considered as the "unsafe" energy storage devices since its invention in 1970s [28,29]. Li metal has high reactivity: (1) it only exists as the compounds in nature. (2) The commercial metallic Li is normally produced by electrolysis. (3) Even without moisture, slow deterioration observed at ambient environment still bring numerous technological issues in processing, characterization and commercial applications [30]. When used as the electrode material in batteries, the lowest reduction voltage of Li metal can increase the operating voltage. On a different perspective, the lowest reduction voltage suggests a high electrochemical reactivity, making it unstable interacting with electrolyte leading to two main challenges, i.e., Li dendrite growth and unstable solid electrolyte interface (SEI) [31–33]. Firstly, the Li dendrites, which is caused by the inhomogeneous Li ion (Li$^+$) plating during the cycling process, could penetrate the separator, cause short circuit and ultimately render catastrophe failure of batteries [34–36]. The morphologies of Li dendrites can be mainly divided into three categories: needle-like, tree-like, and moss-like, which strongly depend on the electrolyte composition and current density [37–39]. Various theories/models have been developed to unravel the mechanism of Li dendrites growth, and one of the popular theories claims that the protrusions with large curvature possess a higher electric field on tips sites, which could attract more Li$^+$ for deposition [40,41]. The Li dendrites may even be isolated from the bulk Li metal and become "dead" Li in the subsequent plating/stripping process, which will result the increased resistance and battery degradation and failure [42,43]. Secondly, the unstable SEI layer will make the scenarios even worse. The uncontrolled interfacial reactions between Li surface and electrolyte along with the huge volume variation of Li metal electrode during the Li$^+$ plating/stripping process are the major causes for the unstable SEI layer [44]. The newly deposited Li continuously reacts at the interface and consumes electrolyte and Li metal, which will result in continuous increase of interfacial resistance and decrease of Coulombic efficiency (CE) [45–47]. Till now, tremendous efforts have been devoted in understanding the problems of Li metal electrode to establish an efficient approach to maintain its long-term performance. Zhang and co-workers revealed that under low current density, the major cause for Li metal electrode failure are the powdering and induced polarization, while under higher current density, the short-circuit due to the penetration of Li dendrite leads to the safety concerns [48]. Cui and co-workers found that the nucleation and growth of Li dendrites are temperature-dependent processes, and a dendrites-free electrode can be obtained by elevating temperature from 25 °C to 60 °C [49]. Song et al. studied the dynamic distribution of Li$^+$ by using the operando neutron radiography and static tomography [50]. They concluded that the short circuit of battery is initiated by the Li dendrites growth, which will partially penetrate the separator from anode to cathode, leading to the fluctuation of voltage profiles.

It can be seen that, in LMBs, the electronically insulating and ionically conductive SEI layer plays a crucial role in mitigating the growth of dendritic Li and protecting Li metal from reacting with electrolytes [51,52]. Therefore, tremendous efforts have been devoted in achieving a stable SEI layer, such as electrolyte modification [53,54], separator modification [55–57], novel design of electrode structure [58] and construction of artificial solid electrolyte interphase (artificial SEI) films [16,24]. Among all the methods, constructing a stable artificial SEI film to protect Li metal anode is an emerging and effective approach. In some reports, the terms like "protecting/protection layer/film" are also used to describe these films. For convenience, the "artificial solid electrolyte interphase" or "protecting/protection layer/film" are hereinafter uniformly referred to as "artificial SEI" in the current paper. The artificial SEI films, which can accommodate the volume variation of Li–metal electrode and suppress the Li–dendrite growth, can be mainly divided into two categories: inorganic artificial SEI films like Al_2O_3 [59], garnet-type $Li_{6.4}La_3Zr_{1.4}Ta_{0.6}O_{12}$ [60], Li_3N [61], LiF [62], Li_2S [63] and carbon materials; organic artificial SEI films such as polyethylene oxide [64], Nafion [65], and polyvinylidene fluoride [66]. Different types of artificial SEI films have their own advantages and disadvantages in regulating the electrochemical performance of Li–metal electrodes. The inorganic artificial SEI films show good electrochemical stability, high mechanical modulus and more efficient Li$^+$ diffusion pathways (for some electrolyte components, such as LiF, $LiNO_3$). While the brittle nature of inorganic artificial SEI films make them prone to be ruptured during a huge volume variation of Li metal, leading to the failure of the LMBs, especially under high current density. For organic artificial SEI films, although the mechanical modulus is lower than that of inorganic materials, their superior processability and high flexibility can achieve intimate contact with electrode and allow effective suppression of the dendritic Li growth, thus significantly improving the electrochemical performance [41,67,68].

Recently, several corresponding review articles have summarized the research progress of artificial SEI films from different perspectives. For example, Zhang and co-workers have summarized the research advances on the interfaces between Li metal electrode and liquid/solid electrolyte, including the both native formed SEI films and artificial SEI films [18]. Xu et al. reviewed different fabrication approaches on artificial protecting films of the Li metal electrode that interacting with liquid or solid electrolyte [69]. According to the protection mechanisms of Li–metal electrodes, Qi et al. summarized existing methods for constructing artificial SEI layers on the Li metal anode [70]. Yang and co-workers focus on summarizing the recent key progress of multi-functional interlayer systems for high-performance LMBs, including tackling the shuttling of Li–S battery and the Li–dendrite issue of Li metal anode [71]. Bao and co-workers discussed the polymer designs for advanced battery chemistry, which also covers some polymeric artificial SEI films [72]. With a few reviews involved the artificial SEI films, till now, there is no review focusing on the ionic conducting polymeric artificial SEI films. Considering the significant research interest on ionic conducting polymers and Li–metal electrode, it is a good momentum to
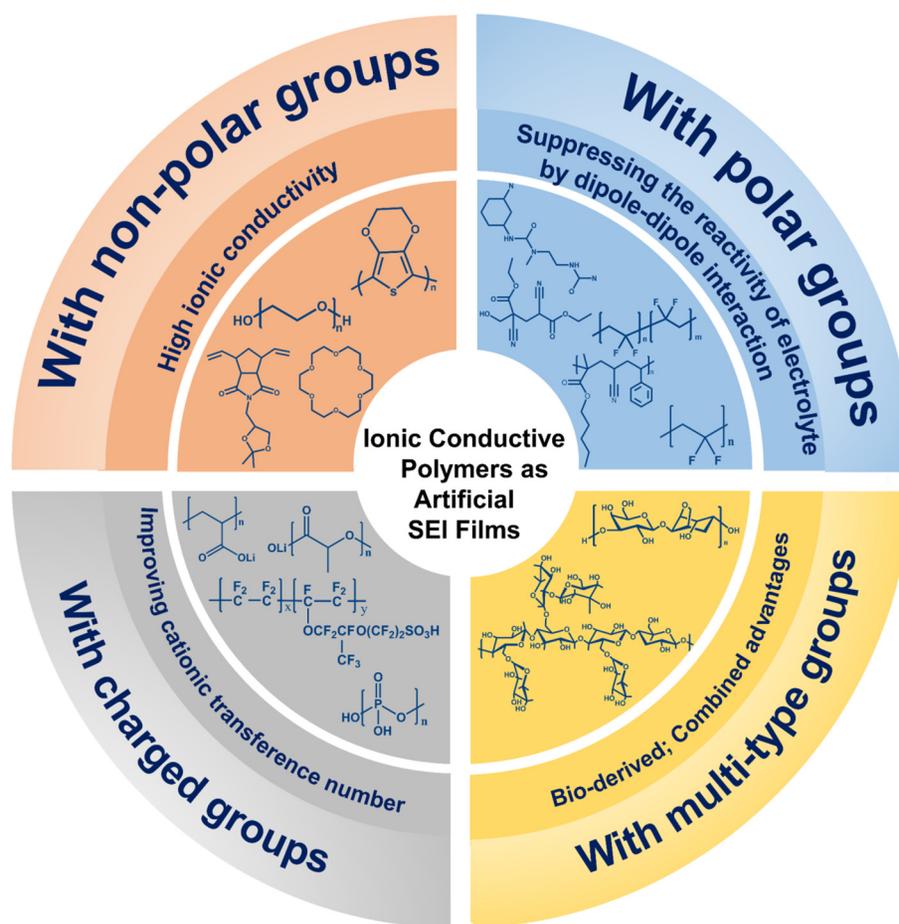
FIGURE 1

Schematic of polymers with different types of ionic conductive groups as efficient artificial SEI films.

review the achievement and present future perspective of ionic conductive polymers as artificial SEI films in LMBs. In this article, as shown in Fig. 1, recent progress of constructing ionic conductive polymers as artificial SEI films, along with their systematic classifications and applied research techniques, will be comprehensively reviewed and summarized. At the end, the future research directions regarding to the rational design of polymeric artificial SEI films in advanced LMBs will also be presented. The deep understandings and design principles of artificial SEI films obtained from the advances of these polymeric protecting films are of significant importance to achieve high-performance LMBs with prolonged lifetime.

Ionic conductive polymers as artificial SEI films in LMBs

The artificial SEI film is defined as a protecting layer on the surface of Li metal electrode that possess the functionalities of SEI. By regulating the Li$^+$ deposition and mechanically suppressing the Li–dendrite growth, the polymeric film can effectively improve the electrochemical performance of the Li–metal batteries [18,70,72]. In 1996, C. Liebenow et al. performed the electrochemical characterization of polymer precoated Li electrodes, whose electrochemical behavior was found being significantly influenced by the passivating layer [73]. The polarization of Li

electrodes was found to vary with the polymer architecture of artificial SEI, and the impedance is highly depending on the immersion time in the electrolyte solution. In 2003, Park and co-workers introduced polymer protected Li metal anodes to the Li–S batteries, which exhibit enhanced electrochemical performance than those with bare Li metal [74]. After that, tremendous efforts have been devoted to constructing polymeric artificial SEI films on Li metal electrodes in different types of LMBs. Generally, to evaluate the performance of an artificial SEI film, Li–Cu cells (artificial SEI coated Cu foil as working electrode and bare Li as counter/reference electrode), Li–Li symmetric cells (artificial SEI coated Li as working electrode and bare Li as counter/reference electrode) and Li–cathode full cells (artificial SEI coated Li or Li deposited on the artificial SEI-modified Cu foil as anode and O$_2$, S, LMO, etc. as cathode) are used. The high CE in Li–Cu cells, low voltage hysteresis in Li–Li symmetric cells and high capacity retention in Li–metal full cells are expected indication of the effective suppression of dendritic Li by artificial SEI film [66].

An ideal artificial SEI film should feature with high chemical/electrochemical stability, high Li$^+$ conductivity and good mechanical robustness/flexibility to accommodate the volume variation and inhibit the penetration of Li dendrites (Fig. 2). The chemical groups and dielectric constant of artificial SEI film along with uniformity and thickness of coating layer are also
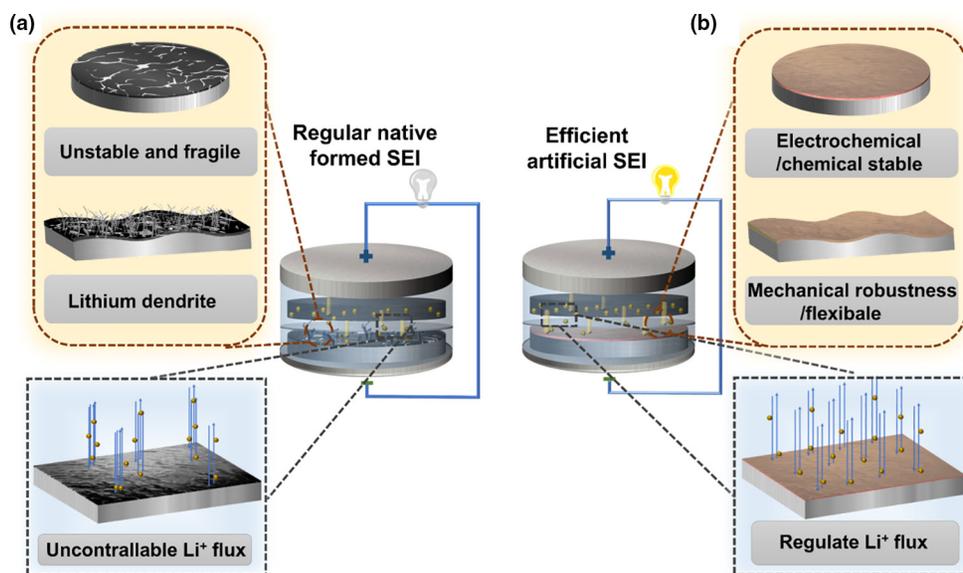
FIGURE 2

Comparative characteristics of (a) regular native formed SEI films and (b) efficient artificial SEI films.

important parameters affecting their electrochemical performance in LMBs [75]. Moreover, with presence of liquid electrolyte, the ionic conductivity of polymeric artificial SEI films is highly dependent on their swelling capability. The high electrolyte uptake and efficient wettability of the artificial SEI films allow fast electrolyte impregnation and high Li+ transport efficiency, which are vital in achieving the full capacity of electrodes [76]. Generally, according to the ionic conductive groups, as shown in Fig. 1, the ionic conductive polymeric artificial SEI films can be classified into four categories: polymers with non-polar groups (—O—), polar groups (—CF, —COOH, —C=O —C≡N, *etc*.), charged groups (Li+ as counter ion) and multi-type of ionic conductive groups. It worth noticing that some polymeric materials do not possess ionic conductive groups but can still provide ionic transfer channels based on the special architecture design, like porous structures [17,25,36], and these types of artificial SEIs will not be included in current review.

Polymers with non-polar ionic conductive groups

Polymers with non-polar ionic conductive groups have been studied for decades, and polyethylene oxide (PEO) is a typical example for this type of polymers. Due to the high ionic conductivity and low cost, the polymers with doped lithium salts have been widely used as the solid electrolytes [77,78]. Under the temperature higher than glass-transition temperature (T > T_g), the Lewis based oxygen (—O—) group serves as ligands to coordinate with Li+, offering necessary solvation energy for the polymer–Li+ complex formation, thus achieving the satisfied ionic conductivity *via* the repeated coordination–dissociation process [79,80]. The ionic conductivities of these polymers are inversely related to their degree of crystallinity. Therefore, suppressing the polymers' crystallinity is essential to enhance the ionic conductivity for the non-polar ionic conducting group containing polymeric artificial SEI films.

After previous demonstration by Liebenow et al. that the PEO modified Li electrode showed lower resistance than pure Li elec-

trode [73], Park et al. applied the PEO-based artificial SEI layer in Li–S batteries [74]. The artificial SEI film on the Li metal surface was obtained using polymerized poly(ethylene glycol) dimethacrylate. The dense artificial SEI film can suppress the growth of dendritic Li, prevent over-charge potential and mitigate side reactions between Li metal anode and soluble polysulfides, thus improving the electrochemical performance.

With unsatisfied artificial SEI performance using PEO itself, formation of PEO (or PEG (polyethylene glycol)) based block copolymer with other functional polymers is a viable approach to develop high-performance polymeric artificial SEI films due to combined advantages from both polymer segments. Poly(3,4 -ethylenedioxythiophene) (PEDOT) with mechanical integrity is a widely studied functional polymer, usually as binder or surface coating material for lithium-ion and Li–S batteries [81–85], while its poor ionic conductivity makes the PEDOT not an ideal candidate as the artificial SEI film. Copolymers of PEO-PEDOT have been designed for improved ionic conductivity. For example, Kim and co-workers reported a PEDOT-*co*-PEG copolymer as the protected layer, and the coated copolymer exhibits high ionic conductivity and strong adhesive properties that can mechanically suppress the growth of dendritic Li during the cycling process [86]. The full cell with copolymer coated Li metal as anode and LiCoO2 (LCO) as cathode exhibits remarkably improved cycling performance with the capacity retention of 87.3% compared with 9.3% for the cell with pristine Li electrode after 200 cycles. Ma et al. also prepared a PEDOT-*co*-PEG copolymer coated Li metal anode that can be applied in Li–S batteries as illustrated in Fig. 3a. The results indicates that the strong adhesion and high ionic conducting properties of PEDOT-*co*-PEG copolymers could effectively inhibit the side reactions between Li anode and Li polysulfides and suppress the dendritic Li growth, thus significantly improving the electrochemical performance of the assembled cells (Fig. 3b) [87]. High adhesion force, good mechanical properties and high conductivity make the PEDOT-*co*-PEG based copolymer a simple and novel polymeric
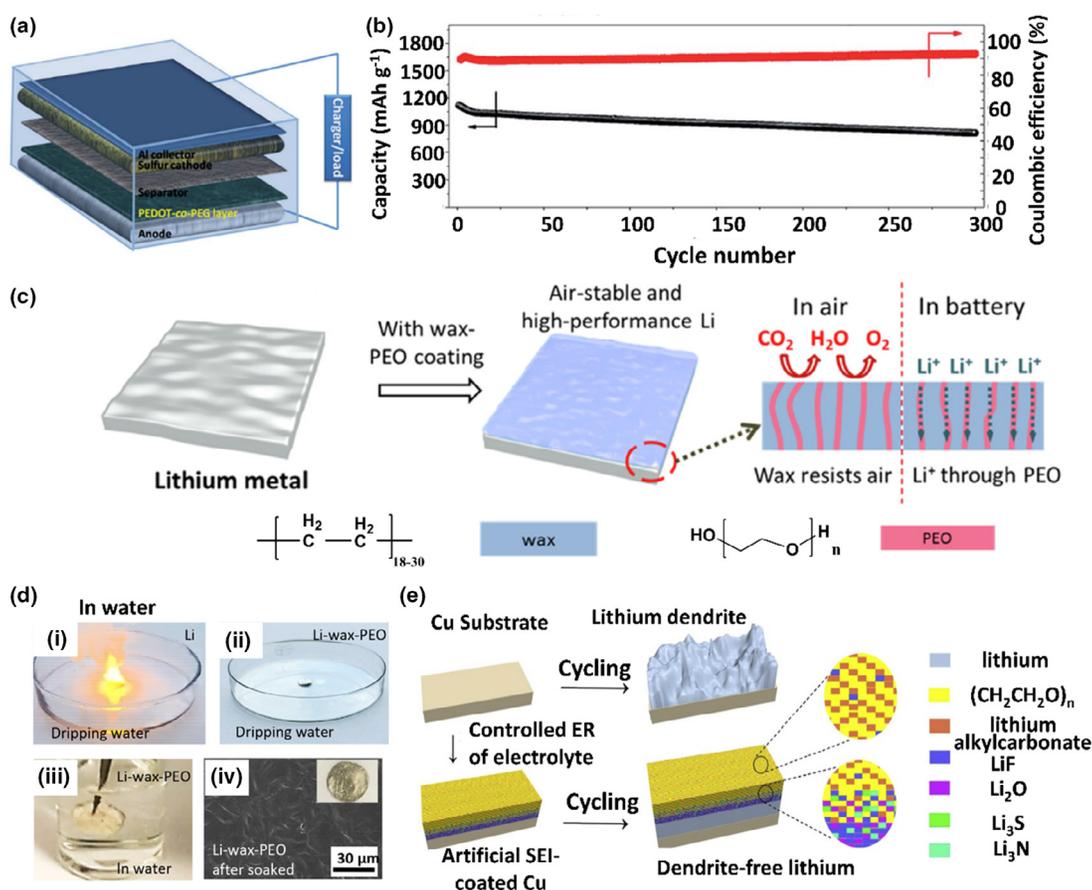
FIGURE 3

(a) Schematic illustration and (b) cycling performance of Li–S cell with PEDOT-*co*-PEG modified Li as anode. Reproduced with permission [87]. Copyright 2014, The Royal Society of Chemistry. (c) Illustration on the wax-PEO coating. (d) The stability demonstration of wax-PEO coated Li and bare Li in water: The optical photos of bare Li (i) and wax-PEO coated Li (ii) when water was dripped on the surface; (iii) the photo when wax-PEO coated Li was soaked in water and (iv) the morphology of wax-PEO coated Li after soaked in water. Reproduced with permission [88]. Copyright 2019, Elsevier. (e) Artificial SEI formation and Li deposition on bare and polymer-coated Cu substrate electrodes. Reproduced with permission [93]. Copyright 2019, Elsevier.

artificial SEI films to protecting Li metal electrode from uncontrolled deposition.

Aside from chemical methods, physical blending to form a PEO based polymer composite is also promising for fabrication of polymeric artificial SEI films. For example, a Li metal electrode featured with an air-stable and waterproof surface using the PEO based composite artificial SEI film (Fig. 3c and d) was also prepared by Yang and co-workers for Li–S battery applications [88]. In the long-cycle test of Li–S cells, the wax-PEO protected Li metal exhibits enhanced cycling performance with a discharge capacity of 776 mAh g^{-1} after 300 cycles. The achievement of polymeric artificial SEI protected Li metal anode with high stability in both air and water is meaningful to lower the requirement of operation circumstances and promote the practical application of LMBs.

To further improve the mechanical performance and transference number of Li$^+$, the ceramic electrolytes have been incorporated to achieve the PEO based inorganic–organic hybrid artificial SEI films. Due to the synergistic effects, the composite artificial SEI films could exhibit high physical/electrochemical stability, flexibility and enhanced ionic conductivity [89–91]. Hu and co-workers developed a hybrid Li$^+$ conducting film comprising the garnet-type ionic conductor Li$_7$La$_3$Zr$_{1.75}$Nb$_{0.25}$O$_{12}$ (LLZNO) and PEO-based polymer to suppress the dendritic Li growth [92]. The dispersed ceramic electrolyte can significantly enhance the mechanical properties and suppress the crystallization of PEO based film, which will also contribute to the efficient Li$^+$ transfer. The electrochemical test indicated that enhanced cycling stability and low voltage hysteresis was achieved in Li–Li symmetric cells, due to the protection of hybrid membrane. The full cell with LFP as cathode and hybrid film modified Li as anode exhibits high retention capacity of ~150 mAh g^{-1} after 100 cycles. Similarly, by controlling electrochemical reduction of lithium bis(trifluoromethanesulfonyl)imide/dimethyl ether-lithium nitrate (LiTFSI/DME-LiNO$_3$), a dual-layer structured hybrid artificial SEI film with organic PEO and Li alkylcarbonate as outer layer and inorganic species such as LiF, Li$_3$N and Li$_2$S as inner layer can also be constructed as displayed in Fig. 3e [93]. Due to the high flexibility and mechanically robustness of the hybrid artificial SEI film, the Li–Cu cells have remarkably improved CEs under various current densities.

Other inorganic materials have also been reported to blend with PEO to form a hybrid artificial SEI film. For example, a hybrid artificial SEI film, derived from the physically

5

compositing of graphene–polydopamine and PEO, can efficiently prohibit side reactions between redox mediators and Li metal electrode (Fig. 4a) [91]. With the synergistic effect from both components, as shown in Fig. 4b, a high CE of >80% was obtained after 150 cycles in an assembled Li–O$_2$ cell. Moreover, direct fabrication of PEO based film from ethylene glycol monomers is also a feasible method to achieve PEO based hybrid artificial SEI films. As illustrated in Fig. 4c, using the molecular layer deposition (MLD) method, Chen et al. demonstrated the in situ formation of hybrid artificial SEI film with highly cross-linked ether units coating around the aluminum framework on the Li metal surface [94]. Possessing both high ionic conductivity and mechanical robustness derived from the organic and inorganic components, respectively, the hybrid artificial SEI film can effectively stabilize Li metal anode against dendritic Li growth and minimize the side reactions in both Li–Li symmetric cell and Li–S cell. As shown in Fig. 4d, with 2.5–3 mg cm^{-2} sulfur loading, a discharge capacity of ~815 mAh g^{-1} can still be retained after 300 cycles under the current density of 0.5 C for a Li–S cell.

Many other polymers with ionic conductive non-polar groups, such as 18-Crown-6 [95], poly(1,3-dioxolane) (polyDOL) [96], and dimethyl-1,3-dioxolane [97] have also been investigated as the artificial SEI films to improve the electrochemical performance of Li metal electrode. Wu and co-workers demonstrated a 18-Crown-6 and PVDF based composite polymeric artificial SEI film (Fig. 5a) [95], which was directly coated onto the surface of Li metal anode via a spin-coating method with the thickness of 5.1 μm. High electrochemical stability and dielectric constant of PVDF along with high ionic conductivity of 18-Crown-6 synergistically make the composite artificial SEI layer efficiently suppress the growth of dendritic Li. As displayed in Fig. 5b, the assembled Li–Cu cells exhibits the CEs of above

97.38% after more than 200 cycles at the current density of 0.2 mA cm^{-2} and 95.61% after 90 cycles at the current density of 0.5 mA cm^{-2}. Moreover, enhanced cycling stability and reduced resistance can also be obtained in Li–S full cells (Fig. 5c). Utilization of another cyclic ether group, i.e., dimethyl-1,3-dioxolane, Wang and co-workers reported a novel skin-grafting strategy to stabilize the Li metal electrode using the poly((N-2,2-dimethyl-1,3-dioxolane-4-methyl)-5-norbornene-exo-2,3-dicarboximide) as shown in Fig. 5d [97]. Different from most of the polymeric artificial SEI films reported previously, the demonstrated polymer is an electrochemically active materials, and the high volume fraction of cyclic ether group in the polymer chains has high affinity with the Li metal surface, which can effectively regulate the Li$^+$ plating/stripping behavior during the repeated charge and discharge process. Li metal anode with this grafted skin showed significantly higher CE and improved cycling stability in the Li–Cu and Li–Li symmetric cells. Moreover, when paired with LFP or NMC cathode materials, capacity retentions of 90.4% and 90.0% can be achieved, respectively, after 400 cycles, which are in dramatic contrast to the cells with bare Li metal anodes. DOL is an organic solvent of electrolyte that can be reduced and electrochemically polymerized on the Li metal to form an elastic protection layer, while the poor anodic stability of DOL will lead to unstable SEI layer and increased viscosity. Formation of organic/inorganic hybrid film is an effectively approach to address this issue. For example,

Kozen et al. reported a hybrid organic/inorganic artificial SEI film via the atomic layer deposition (ALD) and electrochemical polymerization of DOL to composite with LiPON on the Li metal (Fig. 5e) [96]. Due to the high flexibility of organic "poly-DOL" and electrochemical stability of inorganic lithium phosphorous
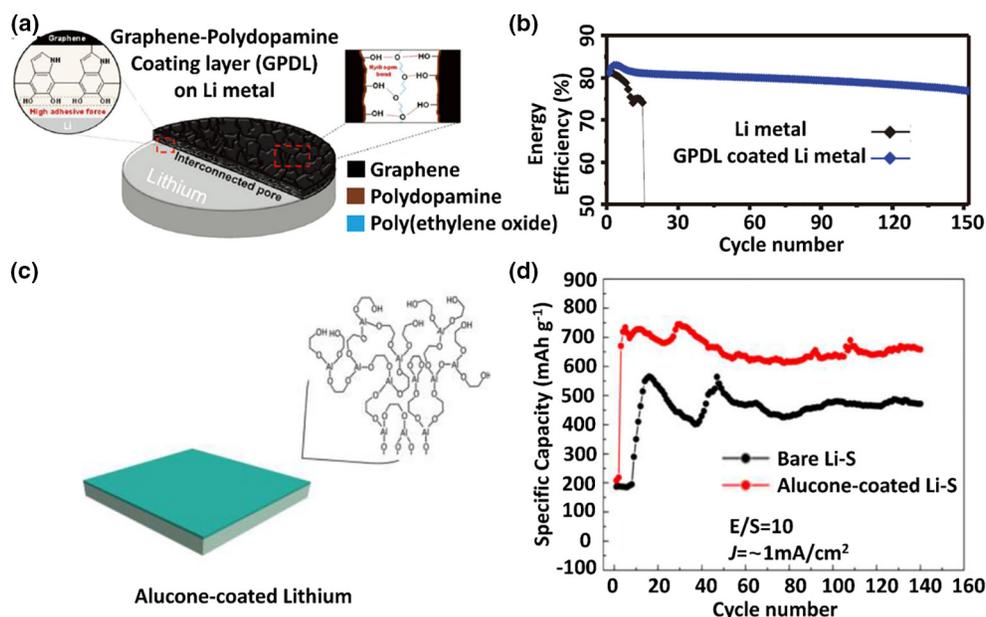
FIGURE 4

(a) Schematic illustration of graphene–polydopamine composite layer coating process. (b) Energy efficiencies of the Li–O$_2$ cells with and without artificial SEI film coated Li as anodes. Reproduced with permission [91]. Copyright 2017, WILEY-VCH Verlag GmbH & Co. KGaA, Weinheim. (c) Illustration of alucone coated Li metal electrode. (d) Cycling performance of Li–S cells with bare and alucone-coated Li as anode. Reproduced with permission [94]. Copyright 2018, American Chemical Society.
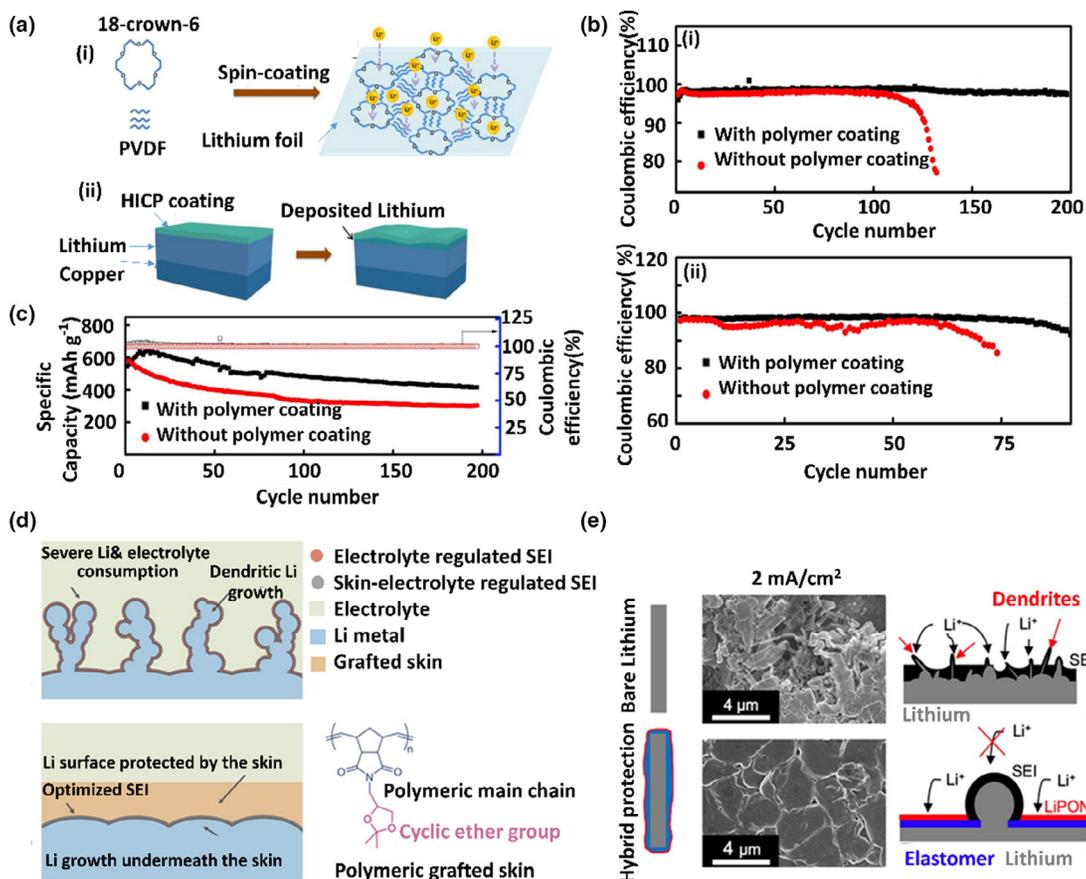
FIGURE 5

(a) (i) Formation of the protective layer and (ii) corresponding electrodes. (b) The CEs of the Li–Cu cell at the current density of (i) 0.2 mA cm^{-2} and (ii) 0.5 mA cm^{-2}. (c) Cycling performance of Li–S cells with or without polymer coating at 0.2 C. Reproduced with permission [95]. Copyright 2019, Elsevier. (d) Illustration of different interfacial chemistries of Li metal with and without artificial SEI films. Reproduced with permission [97]. Copyright 2017, American Chemical Society. (e) SEM images of bare Li metal and protected Li metal electrodes. Reproduced with permission [96]. Copyright 2019, American Chemical Society.

oxynitride (LiPON), the hybrid artificial SEI layer can effectively suppress the Li dendrites formation and stabilize Li metal anode up to 300 and 110 cycles at the current densities of 1 mA cm^{-1} and 2 mA cm^{-1}, respectively, in Li–Li symmetric cells.

In summary, as traditional polymeric electrolyte component, PEO-based polymers can efficiently protect Li metal anode to achieve significantly improved electrochemical performance, while only PEG (or PEO) is far from an ideal artificial SEI film. Copolymerizing or compositing with other organic/inorganic materials for improved the chemical/electrochemical stability, mechanical robustness and flexibility allows high-performance artificial SEI films in LMBs. Although ionic conductive polymers with other non-polar groups have not be studied thoroughly, they also show unique advantages in improving electrochemical performance of LMBs. For example, synthesis of ionic conducting polymers using the cyclic ether groups with tunable ring size may allow additional control over the transport of Li$^+$ in the artificial SEI layer.

Polymers with polar ionic conductive groups

Polymer materials with polar groups can conduct Li$^+$ *via* the physical interactions between the polar groups and Li$^+$. The polar groups, such as amide group (—NHCO—) [98], nitrile group

(—CN) [99], hydroxy group (—OH) [100] and polar carbon–fluorine units (—CF) [66], can redistribute Li$^+$ flux and lead to a relatively homogenous Li$^+$ deposition on metal surface, thus improving the electrochemical performance of Li–metal anode.

As illustrated in Fig. 6a, Sun and co-works introduced an ultra-thin "polyurea" film formed from ethylenediamine and 1,4-phenylene diisocyanate to protect Li metal anode *via* the MLD method [98]. The polar urea groups on the "polyurea" can homogenize the Li$^+$ flux and lead to a uniform Li$^+$ plating/stripping. As a result, the Li metal anode with this "polyurea" as the protective layer can significantly prolong the lifetime of Li–Li symmetric cells (about three times longer than bare Li anode). In full cells with LFP as cathode, enhanced cycling stability and rate capability have also been demonstrated. The X-ray photoelectron spectroscopy (XPS) results showed that the surface layer of protected Li anode contained much higher content of LiF and lower content of Li$_2$O and Li$_2$CO$_3$ than that of the bare Li. This benefits the formation of a stable and mechanical robust SEI layer that can effectively suppress the dendritic Li growth. It was also pointed out that the polar groups (—NHCONH—) in the "polyurea" have strong hydrogen bonding with Li salt, such as Li$_2$O, Li$_2$CO$_3$ and LiF, and the stable LiF could be preferentially formed after the decomposition of Li–N–H–F species.

7
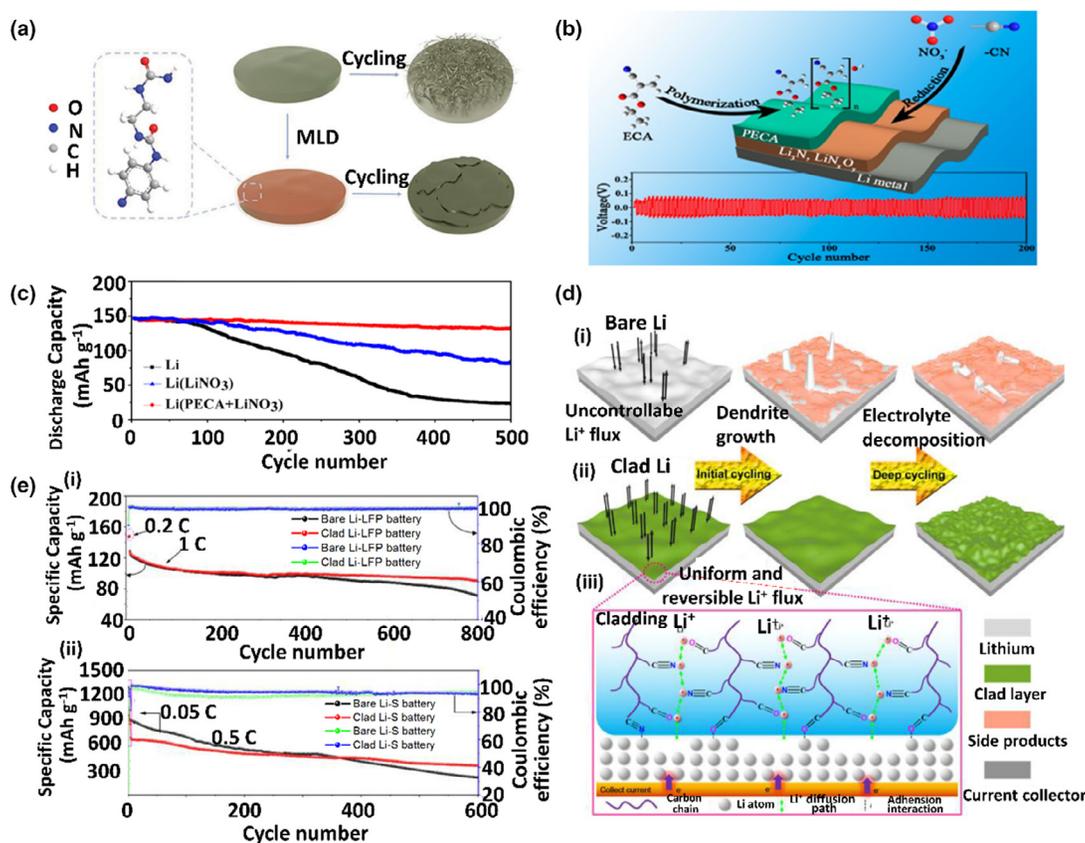
FIGURE 6

(a) Illustration of dendritic lithium growth with and without polyurea coating on Li electrodes. Reproduced with permission [98]. Copyright 2019, WILEY-VCH Verlag GmbH & Co. KGaA, Weinheim. (b) The artificial SEI layer based on in situ polymerization of ethyl α-cyanoacrylate precursor with LiNO$_3$ additive. (c) Cycling performance of the Li–LFP cells with different anodes. Reproduced with permission [101]. Copyright 2017, American Chemical Society. (d) Schematic illustrations on the repeated plating/stripping without (i) and with (ii) P(BMA–AN–St) regulation. (iii) is the local magnified view of cladding Li. (e) Cycling performance of (i) Li–LFP cells at 1 C and (ii) Li–S cells at 0.5 C with and without clad Li as anodes. Reproduced with permission [99]. Copyright 2019, American Chemical Society.

The —CN and —NO$_3^-$ groups can react with Li metal to form a nitrogenous inorganic interfacial layer during the Li$^+$ plating/stripping process, and the formed artificial SEI layer can effectively facilitate Li$^+$ transfer, regulate Li$^+$ flux and suppress side reactions on the Li metal surface. Chen and co-workers designed an artificial SEI film with abundant —CN and —NO$_3^-$ (from the LiNO$_3$ additive) groups via in situ polymerization of ethyl α-cyanoacrylate precursor [101]. The flexibility of poly (ethyl α-cyanoacrylate) (PEAC) layer can accommodate the volume change of Li metal during the cycling process, where the polar groups can effectively facilitate the homogeneous distribution of Li$^+$ and stabilize the Li metal interface layer as illustrated in Fig. 6b. As a result, enhanced electrochemical performance with the capacity retention of 93% after 500 cycles at the current rate of 2 C can be obtained for the cells with protected Li metal anode and LFP cathode (Fig. 6c). Similarly, simultaneous regulation of Li$^+$ flux and surface activity was realized by the surface coating of a terpolymer, poly(butylmethacrylate–acrylonitrile–styrene) (P(BMA–AN–St)) reported by Wang et al. as shown Fig. 6d [99]. With this terpolymer as the artificial SEI film, stable cycling performance, prolonged cycle lifespan and reduced interfacial resistance can be obtained in both Li–LFP and Li–S cells (Fig. 6e).

Carbon–fluorine (—CF) group is another polar ionic conducting unit that allows the constructed polymeric artificial SEI film to have uniform Li$^+$ deposition. For example, Ishihara and co-workers demonstrated that Li–O$_2$ cells with poly(vinylidene fluoride-co-hexafluoropropylene) (PVDF–HFP) as artificial SEI film of Li electrode showed decreased interfacial resistance and enhanced cycling stability [102]. Further study showed that preparation of a hybrid protective layer (CPL) by compositing PVDF–HFP with Al$_2$O$_3$ nanoparticles can enhance the mechanical robustness of artificial SEI that can effectively suppress the initiation and growth of dendritic Li. As shown in Fig. 7a, the Li–O$_2$ cell, in which Li metal electrode is uniformly covered with this hybrid layer, retained a stable discharge capacity of 1000 mAh g^{-1} at the 80th cycle vs a rapid capacity fading after 40 cycles for that with bare Li [102]. The hybrid artificial SEI film was further evaluated in Li–LCO cells, and an excellent cycling stability with the capacity retention of 91.8% after 400 cycles at 1 mA cm^{-2} can be obtained (Fig. 7b) [103]. Huang and co-workers designed a soft–rigid hybrid protective layer with the inorganic ionic conductive component LiF and organic component PVDF–HFP (Fig. 7c i–iii) [21]. The constructed artificial SEI film possesses favorable attributes such as high mechanical mod-
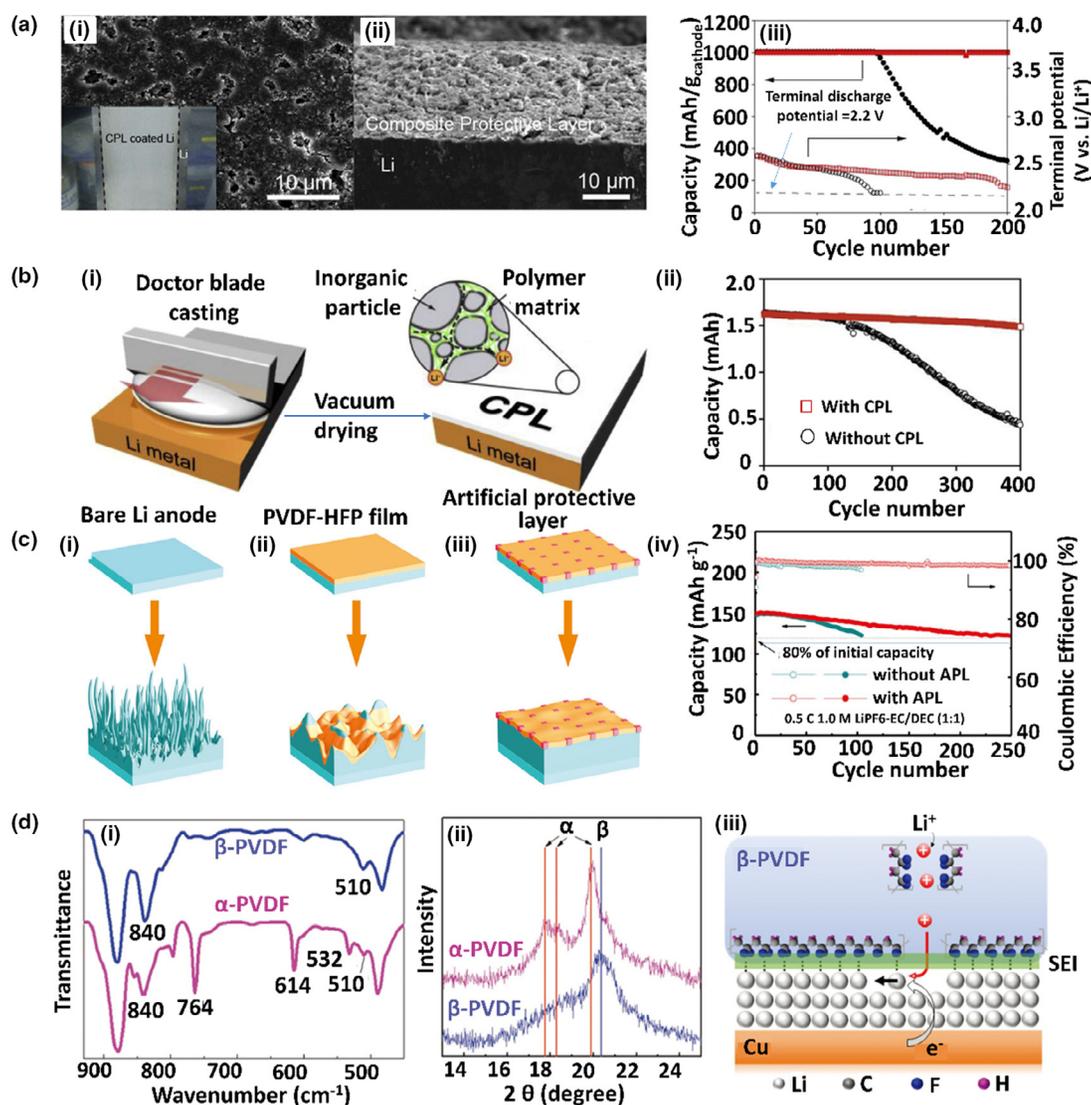
FIGURE 7

(a) (i) SEM morphologies. (ii) Cross-sectional image of artificial SEI-coated Li electrodes. (iii) Cycling performance of Li–O$_2$ cells with bare and artificial SEI-coated Li as anodes. Reproduced with permission [124]. Copyright 2014. Elsevier B.V. (b) (i) Schematic illustration of the composite artificial SEI film fabrication process. (ii) Electrochemical performance of Li–LCO cells with bare and artificial SEI-coated Li as anodes. Reproduced with permission [103]. Copyright 2015. Elsevier B.V. (c) Schematic illustrations of Li deposition on (i) bare Li, (ii) PVDF-HFP film coated Li and (iii) APL composed of organic PVDF-HFP and inorganic LiF coated Li. (iv) Electrochemical performance of Li–LFP cells with bare and PVDF-HFP film coated Li as anodes. Reproduced with permission [21]. Copyright 2018. WILEY-VCH Verlag GmbH & Co. KGaA, Weinheim. (d) (i) FTIR spectra (ii) and XRD patterns of the β- and α-PVDF. (iii) Schematic illustration of Li deposition and preferential diffusion pathways for Li$^+$ due to the β-PVDF. Reproduced with permission [66]. Copyright 2017, WILEY-VCH Verlag GmbH & Co. KGaA, Weinheim.

ulus, high ionic conductivity and excellent compatibility with Li metal surface. In Li–Li symmetric cells, the composite AESI film contributed to improved CE and prolonged cycle life. Fig. 7c iv shows superior cycling performance with capacity retention of 80% after 250 cycles in full cells with LFP as paired cathode.

Although —CF group containing polymers can suppress the dendrite Li growth and protect the Li anode from erosion, it should be noticed that the phase behavior of PVDF significantly affect its polarity and coating behavior. Luo et al. demonstrated that the electrochemical performance of the PVDF coated lithium electrode is closely related with its molecular conformation [66]. The α phase with a *trans–gauche–trans–gauche* conformation presents the nonpolar nature, while the β phase with all trans conformation is the most polar form [104]. Under differ-

ent drying speeds after the solution casting of PVDF on the Li metal surface, different phases can be obtained as displayed in the FTIR spectra and XRD patterns shown in Fig. 7d i and ii, respectively. Compared with α-PVDF, β-PVDF as the protected layer can suppress the Li dendrites growth and enhance the cycling stability in a much more efficient manner due to its highly polar nature. The results have been well validated by the assembled Li–Cu and Li–LFP cells in which the β-PVDF protected Li–metal electrode exhibited an excellent cycling performance comparing with rapid capacity fading of the α-PVDF coated one.

In summary, the advantages of polar groups as ionic conducting units in polymeric artificial SEI lie in the following aspects: (1) the interaction between the polar groups and Li$^+$ promote

the controlled layer-by-layer deposition of Li+, thus suppressing the Li dendrites growth; (2) the polar groups provide preferential diffusion paths to achieve rapid Li+ plating/stripping that can enhance the rate capability; (3) with the presence of polar groups, the artificial SEI film exhibited an enhanced interactions with Li metal surface, which also mitigate the side reactions with electrolyte.

Polymers with charged ionic conductive groups

Polymers with charged groups (Li+ as counter ion) possessing high ionic conductivity, wide electrochemical window and superior chemical/electrochemical stability, have been extensively studied as solid and gel electrolyte [105–108]. In recent years, considerable efforts have also been devoted to utilization of polymers with charged groups as artificial SEI films for protection of Li metal electrode. In this aspect, with anions covalently attached to the polymer backbones, a single-ion conducting polymer electrolyte can be obtained with only cation being mobile, and the dissociation capability between Li+ and counter ion should play a vital role when used as the artificial SEI film in LMBs.

Lithium polyacrylate (LiPAA), with superior binding capability and Li+ conductivity, has been widely studied as the polymer binder for high-capacity electrode in LIBs [7,109]. Recently, Guo and co-workers designed a "smart" LiPAA based artificial SEI layer with high elasticity that can accommodate the Li deformation during the repeated Li+ plating/stripping process by self-adapting interface regulation (Fig. 8a) [110]. The atomic force microscope (AFM) results demonstrate that the Li+ plating/stripping process can generate dendritic Li on the surface of bare Li electrode, while a smooth surface was observed with the LiPAA as the artificial SEI protected film. The efficient binding capability and high ionic conductivity play important roles in the formation of self-adapting artificial SEI film on the Li metal surface that achieving enhanced electrochemical performance (Fig. 8b and c). By integrating dynamic flowability, efficient single-ion conduction, and electrolyte-blocking performance into a single matrix, Bao and co-workers designed a dynamic single-ion-conductive (DSN, the chemical structure of FTEG is shown in Fig. 8d) artificial SEI film as shown in Fig. 8e [104]. The flowability and single-ion conductivity come from the tetrahedral $Al(OR)_4^-$ (R = soft fluorinated linker) centers, which act as both dynamic bonding motifs and counter anions. The constructed artificial SEI films show many features such as fast ion transport, conformal protection, and parasitic reaction mitigation that can guide homogenous Li+ deposition, mitigate side reactions and hinder electrolyte penetration. As shown in Fig. 8f, the full cell with coated Li as anode and commercial $LiNi_{0.5}Mn_{0.3}Co_{0.2}O_2$ (NMC 532) (~95% active material, 2 mAh cm^{-2} loading) as cathode delivers a discharge capacity of 132.9 mAh g^{-1} after 160 cycles under the current density of 1 C.

With high ionic conductivity and good electrochemical stability, lithiated Nafion may also be an ideal candidate as artificial SEI film, while the unsatisfied mechanical performance limited the efficient suppression of lithium dendrite growth if used alone. Construction of the hybrid Nafion based artificial SEI films with inorganic materials has been demonstrated an efficient

approach with improved performance. For example, Li et al. fabricated a lithiated Nafion/LiCl composite interface (NLI) on the Li metal anode via a simple dip-casting approach [111]. The lithiated Nafion can provide efficient Li+ transfer channels and good interfacial contact, and the additional LiCl fillers can significantly improve its mechanical modulus (6.12 GPa, Fig. 9a). The synergistic effect of the organic/inorganic components enables the constructed artificial SEI film to effectively suppress the dendritic Li growth, promote uniform Li+ flux and stabilize Li metal surface. In Li–Cu cells, the NLI-coated electrode exhibits much higher CE and longer cycling lifetime under various operating conditions than the bare Li metal electrode. Moreover, enhanced electrochemical performance was also obtained in full cells when the protected Li metal electrode paired with LFP (Fig. 9b). It has been reported that the sulfonate groups (exist in Nafion) can suppress the anion hopping in Li–S batteries, thus reducing the side reactions between Li metal anode and polysulfides [112–114]. Based on this concept, as shown in Fig. 9c, Chen and co-workers reported a lithiated Nafion/TiO2-coated Li metal electrode that can be used in Li–S cells [115], and it was found that doping of TiO2 nanoparticles can improve the ionic conductivity of Nafion (~10 times improvement) (Fig. 9d). The scanning electron microscope (SEM) images of Li electrodes after 100 charge–discharge cycles show that for Nafion/TiO2-coated Li, a smooth surface can be observed, indicating the integrity of the Li anode during the repeated cycling process. The presence of inorganic TiO2 can significantly improve the mechanical robustness of result artificial SEI film, leading to a uniform Li+ deposition and hence excellent cycling stability (see Table 1) and superior rate capability of the protected Li metal electrode. The electrochemical impedance spectroscopy (EIS) and SEM results demonstrate the decreased interfacial resistance and smooth surface for the protected Li metal electrode, which is consistent with the enhanced electrochemical performance. Aside from the Li–S cells, lithiated Nafion-based hybrid artificial SEI, i.e. lithiated Nafion-Al2O3, was also constructed for the application of Li–O2 cells [65]. As illustrated in Fig. 10a, with this protective layer, Li metal electrode exhibits reversible oxygen reduction and evolution, indicating its effectiveness in mitigating the dendritic Li growth and other side reactions (Fig. 10b).

Instead of simple blending Nafion with other inorganic materials, dual-layer structured hybrid artificial SEI film with Al-doped $Li_{6.75}La_3Zr_{1.75}Ta_{0.25}O_{12}$ (LLZTO) as bottom layer and Nafion as top layer was also fabricated (LLZTO/Li–Nafion, LLN) [29]. Taking advantages of high mechanical strength and efficient Li+ diffusion channels provided by ceramic electrolyte along with the elasticity of Nafion, the dual-phase protected layer can effectively protect Li metal surface from Li dendrite growth as illustrated in Fig. 10c. The result shows that these two layers in LLN were tightly attached with each other, which ensure the efficient regulation of Li+ transfer behavior. The assemble full cell with LLN-coated Li as anode and LFP as cathode shows a capacity retention of 87.4% after 150 cycles. For the pristine Li electrode, sharp capacity decrease can be observed after 60 cycles, and after reassembled with fresh Li anode, the discharge capacity can recover to 120 mAh g^{-1}. This interesting demonstration indicates that the deterioration of Li metal anode is the major factor leading to capacity fading of LMBs.
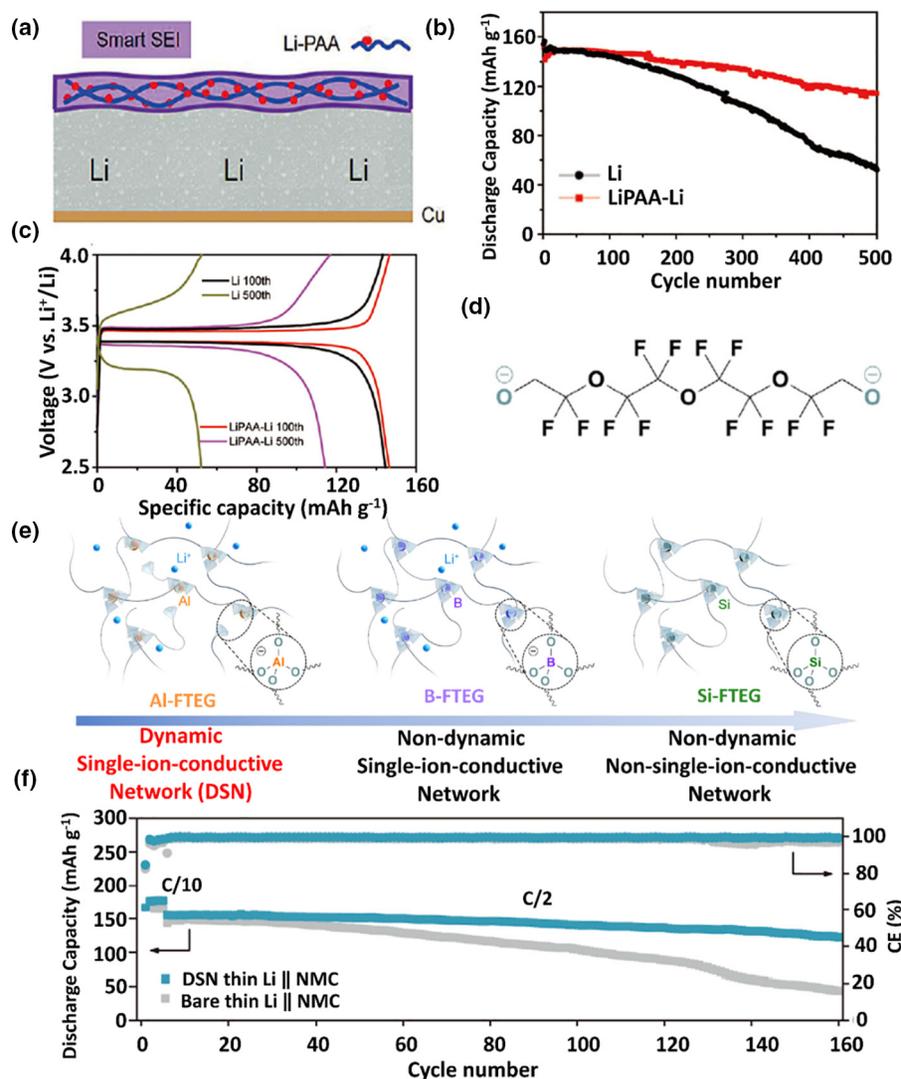
FIGURE 8

(a) Schematic illustration of the "smart" LiPAA based artificial SEI layer. (b) Cycling performance and (c) discharge–charge curves of Li–LFP cells with bare and "smart" LiPAA coated Li–metal electrodes. Reproduced with permission [110]. Copyright 2018. V Wiley-VCH Verlag GmbH & Co. KGaA, Weinheim. (d) Chemical structure of FTEG. (e) Conceptual sketch of Al-FTEG, B-FTEG and Si-FTEG (FTEG: 1H,1H,11H,11H-perfluoro-3,6,9-trioxaundecane-1,11-diol). (f) Cycling performance of Li–NMC cells with bare and DSN-coated Li as anodes. Reproduced with permission [104]. Copyright 2018. Elsevier Inc.

The aforementioned polymers with charged groups are all pre-synthesized with Li^+ conductivity, and the in situ formation of ionic conducting charged polymer films is also an alternative approach. Liu et al. fabricated a Li silicate protected layer on Li metal surface *via* the simple vapor deposition method [116]. As displayed in Fig. 11a and b, the Li foil is exposed to the mixed vapor of 3-mercaptopropyl trimethoxysilane and tetraethoxysilane, and after heat treatment, a thin layer of Li silicate (Li_xSiO_y) can be formed on the Li surface. The Li_xSiO_y coated-Li enabled significantly improved cycling performance in Li–LFP and Li–S cells. Besides, by in situ reaction of Li metal with polyphosphoric acid (PPA), an artificial SEI film with good chemical stability, high Young's modulus and ionic conductivity can also be obtained as shown in Fig. 11c [117]. In the batteries with bare Li metal as electrode, repeating breakage and reformation of SEI film will consume the electrolyte and render the corrosion of Li metal. While, LiPPA (lithium polyphosphate) based artificial

SEI film can effectively reduce the side reactions between Li metal and electrolyte, thus improving its electrochemical performance (Fig. 11d). Moreover, the LiPPA‖Li symmetric cell exhibits a stable cycling performance after 600 h without short circuiting compared with the rapid failure of Li–Li symmetric cells only after 55 h. Partial hydrolysis of the biodegradable polylactic acid (PLA) with Li may also result a charge-group containing polymer. Recently, Guo and co-workers prepared an ionic group containing artificial SEI layer *via* in situ reaction between Li metal and PLA to improve the electrochemical behavior of Li metal electrode (Fig. 11e) [118]. The formed LiPLA based artificial SEI layer shows highly rebound resilience and mechanical strength that can effectively regulate the Li^+ plating/stripping behavior, achieving excellent cycling stability in the assembled full cells with LFP or Li–LiNi$_{3/5}$Co$_{1/5}$Mn$_{1/5}$O$_2$ as cathodes (See Table 1).

With Li^+ as counter ion, polymeric artificial SEI films with charged groups as ionic conductive units are promising in
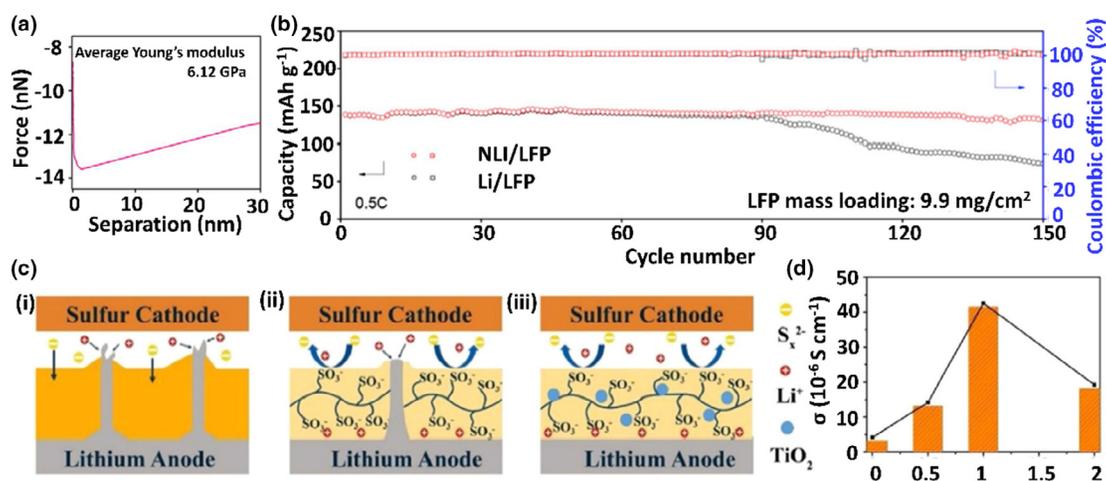
FIGURE 9

(a) The force–distance curve and corresponding fitting Young's modulus. (b) Cycling performance of the cells with and without artificial SEI film modified Li as anodes in Li–LFP cells. Reproduced with permission [111]. Copyright 2018, Elsevier B.V. (c) Schematic illustration of Li–S batteries with different metal Li anodes: (i) pristine Li metal. (ii) Nafion-coated Li. (iii) Nafion/TiO_2-coated Li. Reproduced with permission. (d) Ionic conductivity of Nafion/TiO_2 composites with different contents of TiO_2 [115] Copyright 2018. Wiley-VCH Verlag GmbH & Co. KGaA, Weinheim.

improving the electrochemical performance of LMBs due to their superior binding capability and Li^+ conductivity. Moreover, compositing with inorganic materials such as Al_2O_3, TiO_2 and Li salts to improve the mechanical strength and ionic conductivity or in situ formation of charged group containing polymeric layer on Li metal surface are demonstrated being viable approaches to fabricate effective artificial SEI films for enhanced electrochemical performance of LMBs.

Polymers with multi-type ionic conductive groups

As discussed earlier, polymers with different types of ionic conductive groups have their own advantages. Due to the high ionic conductivity, polymers with non-polar groups, like PEO, have been studied for decades as solid/gel electrolyte, which provided the mature experience for polymeric artificial SEI films in LMBs. At the same time, the polymers with polar or charged groups have their unique advantages: the polar groups can effectively inhibit the movement of Li^+ toward protrusions induced by the tip effect, suppress the growth of Li dendrites and inhibit the side reactions between Li metal and electrolyte; the polymers with charged groups feature with single cationic conducting nature, and high chemical/electrochemical stability. Therefore, rational design of polymers with multi-type ionic conducting groups is a promising approach to prepare high-performance polymeric artificial SEI films with multi-advantages that can significantly improve the electrochemical performance of LMBs.

With the presence of both non-polar (—O—) and polar group (—OH), polysaccharide is a kind of nature-derived polymer that potentially provides high Li^+ conductivity as artificial SEI film [119]. Agarose (AG), with molecular structure shown in Fig. 12a, is a biopolymer with high ionic conductivity, high elasticity and electrochemical stability, which has been demonstrated as efficient artificial SEI film in LMBs [120]. The capability of fast ion transfer and accommodating volume change could effectively inhibit the growth of dendritic Li and result in a stable interface. With Li deposited on the AG-

modified Cu as anode (Li@AG–Cu) and LFP as cathode, as displayed in Fig. 12b, the Li@AG–Cu‖LFP cell exhibits a capacity retention of 87.1% after 500 cycles, which is much better than 70.9% and 5% for pristine Li anode and Li-deposited Cu anode, respectively. Similar to AG, tamarind seed polysaccharide (TSP), was also employed to construct protective film for a stable and dendrite-free Li metal anode (Fig. 12c) [100]. As displayed in the SEM images in Fig. 12d, the corrosion and uncontrolled dendritic Li of Li metal anode can be effectively inhibited. The Li–Cu and Li–S cells were assembled with TSP protected Li anodes, and both of them showed significantly improved electrochemical performance (Fig. 12e).

Interestingly, the common laboratory used supply-Kimwipe (KW) paper, which is mainly made from cellulose fibers, can also achieve the dendrite-free Li metal surface [121]. With abundant polar and nonpolar functional groups, KWs provide excellent wettability to Li^+ and impede the aggregation of Li^+. Moreover, as illustrated in Fig. 12f, due to the presence of cellulose fibers of KWs, a homogeneous Li^+ distribution along the fibers can be achieved, thus effectively suppressing the outgrowth of Li dendrites and improving the electrochemical performance. As shown in Fig. 12g, in Li–Li symmetric cells, a stable cycling performance under various current densities can be achieved after a long-term cycling process, and studies on the feasibility of KWs in full LMBs is expected.

A composite artificial SEI film using Nafion and PVDF that possess charged and polar groups, respectively, was also developed by Luo et al. [122]. The composite artificial SEI film with hierarchical nanostructure could alleviate the swelling and dissolution problems, provide sufficient mechanical strength to accommodate the volume variation and suppress the Li dendrites growth during the cycling process. It was shown that by using this composite artificial SEI protection layer, the dendritic Li growth of Li anode and polysulfide shutting in assembled Li–S cells can be efficiently suppressed thus improving the electrochemical performance (Fig. 12h and i).

TABLE 1

A summary of reported works on artificial SEI films using ionic conductive polymers for Li metal anodes.

Categories	Materials	Strategies	Electrochemical performance	Electrolytes	Areal capacity (mAh/cm^2)	Thickness	Ref.
NP[a]	Alucone	MLD	~99.5% CE @0.4 mA/cm^2, 160th, Li–Cu 657.7 mAh/g @1 mA/cm^2, 140th, Li–S	1 M LiTFSI, 0.18 M Li$_2$S$_8$, 2 wt % LiNO$_3$ in DOL/DME (v/v = 1:1)	1 ~10	~6 nm	[94]
NP	18-Crown-6 + PVDF	Spin-coating	97.38% CE @0.2 mA/cm^2, 200th, Li–Cu Stable cycling for 149 h @1 mA/cm^2, Li–Li 413 mAh/g @335 mA/g, 200th, Li–S	1 M LiTFSI, 2 wt% LiNO$_3$ in DOL/DME (v/v = 1:1)	0.35 \ \	5.1 μm	[95]
NP	Grafted polymer skin[e]	\	98.3% Avg. CE @0.5 mA/cm^2, 200 cycles, Li–Cu Stable cycling for 300 h @0.5 mA/cm^2, Li–Li 90.4% CR[f] @0.5 mA/cm^2, 400th, Li–LFP 90.0% CR @0.3 mA/cm^2, 400th, Li–NCM 523	1 M LiPF$_6$ in EC[g]/EMC[h]/FEC[i] (v/v/v = 3:7:1)	1.0 1.0 2.0 1.0	0.2 μm 2.2 μm	[97]
NP	PEDOT-co-PEG	Spin-coating	87.3% CR @0.5 mA/cm^2, 200th, Li–LCO	1 M LiClO$_4$ in EC/DMC[j] (v/v = 1:1)	1.0	380 nm	[86]
NP	PEDOT-co-PEG + AlF$_3$	Spin-coating	A sustained cell capacity up to 70 cycles @0.2 mA/cm^2 (limited capacity: 1111 mAh/g), Li–O$_2$	1.0 M LiTFSI in TEGDME[k]	1.0	1.0 μm	[89]
NP	Poly"DOL" + LiPON	EC + ALD	Stable cycling for 280 cycles @1.0 mA/cm^2; 110 Cycles @2.0 mA/cm^2, Li–Li	1 M LiPF$_6$ in EC/DEC[l] (v/v = 1:1)	1.0; 2.0	~815 nm	[96]
NP	GPDL[m]	Drop-casting	Stable cycling for 500 h @0.2 mA/cm^2, Li–Li >80% CR @0.15 mA/cm^2, 150th, Li–O$_2$	0.5 M LiBr, 0.5 M LiTFSI in DEGDME[n]	0.2 0.6	30 μm	[91]
NP	PEGDMA[o]	UV curing	Avg. 270 mAh/g during 100 cycles	TEGDME and LiClO$_4$	\	10 μm	[74]
NP	PEDOT-co-PEG	Immersion method	73.45% CR @335 mA/g, 200th; 815 mA h/g @837.5 mA/g, 300th, Li–S	1 M LiTFSI in DOL/DME (v/v = 1:1)	4.2–5	10 μm	[87]
NP	LLZNO + PEO	Drop-casting	Stable cycling for 1000 h @0.2/0.5 mA/cm^2, Li–Li ~150 mAh/g @34 mA/g, 100th, Li–LFP	1 M LiTFSI in DOL/DME (v/v = 1:1)	1; 1 1.0	8–10 μm	[92]
NP	-(CH$_2$CH$_2$O)$_n$-, lithium alkylcarbonate, LiF, Li$_2$O, Li$_3$N and Li$_2$S	ER[p]	97.5% CE @0.5 mA/cm^2, 350th, Li–Cu 97.5% CR @335 mA/g, 50th, Li–S	1 M LiTFSI, 1 wt% LiNO$_3$ in DOL/DME (v/v = 1:1) 1 M LiTFSI in DOL/DME (v/v = 1:1)	0.5 ~1.7	40 nm	[93]
NP	Wax + PEO	Dip-coating	Stable cycling for 500 h @1 mA/cm^2, Li–Li 776 mAh/g @837.5 mA/g, 300th, Li–S	1 M LiTFSI, 1 wt% LiNO$_3$ in DOL/DME (v/v = 1:1)	1 ~4	30 μm	[88]
P[b]	Poly(ethyl α-cyanoacrylate)	Blade-coating	Stable cycling for 200 cycles @1 mA/cm^2, Li–Li 93% CR @2.08 mA/cm^2, 500th, Li–LFP	1 M LiPF$_6$ in EC/DMC (v/v = 1:1)	1.0 ~1.04	200 μm (doctor blade)	[110]
P	PVDF–HFP	Dip-coating	A sustained cell capacity up to 19 cycles @0.1 mA/cm^2 (limited capacity: 1111 mAh/g), Li–O$_2$	1 M LiTFSI in EC/DEC (v/v = 3:7)	\	300–350 μm	[102]
P	PVDF–HFP + Al$_2$O$_3$	Blade-coating	88.2% CR @2.38 mA/cm^2, 300th, Li–LiMn$_2$O$_4$	1 M LiClO$_4$ in EC/PC[q] (v/v = 1:1)	1.26	270 μm (doctor blade)	[123]
P	PVDF–HFP + Al$_2$O$_3$	Blade-coating	A sustained cell capacity up to 60 cycles @0.2 mA/cm^2 (limited capacity: 1000 mAh/g), Li–O$_2$	1.0 M LiClO$_4$ in TEGDME	0.8	25 μm	[90]

TABLE 1 (CONTINUED)

Categories	Materials	Strategies	Electrochemical performance	Electrolytes	Areal capacity (mAh/cm²)	Thickness	Ref.
P	PVDF–HFP + Al$_2$O$_3$	Blade-coating	A sustained cell capacity up to 80 cycles @0.1 mA/cm^2 (limited capacity: 1000 mAh/g), Li–O$_2$	1.0 M LiTFSI in TEGDME	0.5	20 μm	[124]
P	PVDF–HFP + Al$_2$O$_3$	Blade-coating	91.8% CR @1 mA/cm^2, 400th, Li–LCO	1 M LiClO$_4$ in EC/PC (v/v = 1:1)	1	25 μm	[103]
P	β-PVDF	Blade-coating Drop casting	∼98% CE @1 mA/cm^2, 200th, Li–Cu 94.3% CR@ ∼0.2 mA/cm^2, 200th, β-PVDF @Cu‖LFP	1 M LiTFSI, 3 wt% LiNO$_3$ in DOL/DME (v/v = 1:1)	0.5 ∼0.68	4 μm 300 μm	[66]
P	Polyurea	MLD	Stable cycling for 1000 h @0.5 mA/cm^2; 160 h @1 mA/cm^2 ; 200 h @3 mA/cm^2; 420 h @1 mA/cm^2, Li–Li 120 mAh/g @0.8 mA/cm^2, 200th, Li–LFP	1 M LiPF$_6$ in EC/DEC/DMC (v/v/v = 1:1:1)	0.5; 1; 1; 2 0.8	∼250 μm	[98]
P	P(BMA–AN–St)	Immersion method	Stable cycling for 1100 h @0.5 mA/cm^2, Li–Li 90 mAh/g @0.8 mA/cm^2, 800th, Li–LFP 53% CR @∼1.2 mA/cm^2, 600th, Li–S	1 M LiTFSI in DOL/DME (v/v = 1:1) 1 M LiPF$_6$ in EC/EMC/DEC (v/v/v = 1:1:1) 1 M LiTFSI in DOL/DME (v/v = 1:1)	1 ∼0.4 ∼2.3	∼4 μm	[99]
P	PVDF-HFP + LiF	Blade-coating	97.2% (Avg.) @0.5 mA/cm^2, 120th, Li–Cu Stable cycling for 200 h @2.0 mA/cm^2, Li–Li 80% CR @0.378 mA/cm^2, 250th, Li–LFP	1 M LiTFSI in DOL/DME (v/v = 1:1) 1 M LiTFSI in DOL/DME (v/v = 1:1) 1 M LiPF$_6$ in EC/DEC (v/v = 1:1)	1.0 1.0 0.756	∼12 μm	[21]
C^c	Li$_x$SiO$_y$	Vapordeposition technique	Stable cycling for 500 h @0.5 mA/cm^2, Li–Li 103.6 mAh/g @0.425 mA/cm^2, 500th, Li–LFP 693 mAh/g @1.005 mA/cm^2, 500th, Li–S	1 M LiPF$_6$ in EC/DEC (v/v = 1:1) 1 M LiPF$_6$ in EC/DEC (v/v = 1:1) 1 M LiTFSI in DOL/DME (v/v = 1:1)	1.0 0.85 3.35	>20 nm	[116]
C	Nafion + TiO$_2$	Drip-coating	64.4% CR @0.167 mA/cm^2, 100th, Li–S	1 M LiTFSI in DOL/DME (v/v = 1:1)	0.836	∼4 μm	[115]
C	Nafion + Al$_2$O$_3$	Drop-casting	Stable cycling for 2000 h @0.2 mA/cm^2; 700 h @0.5 mA/cm^2, Li–Li A sustained cell capacity up to 30 cycles @0.2 mA/cm^2 (limited capacity: 2000 mAh/g), Li–O$_2$	1 M LiTFSI in DEGDME 1 M LiTFSI in TEGDME	0.2; 0.5 \	3 μm	[65]
C	LiPAA	Drip-casting	Stable cycling for 700 h @0.5 mA/cm^2; 250 h @1 mA/cm^2; Li–Li ∼110 mAh/g @\ mA/cm^2, 500th, Li–LFP	1 M LiPF$_6$ in EC/DMC/DEC (v/v/v = 1:1:1) 1 M LiPF$_6$ in EC/DMC/DEC (v/v/v = 1:1:1)	\ ∼0.68	∼20 nm	[110]
C	PPA-Li	Dip-coating	∼150 mAh/g @∼0.26 mA/cm^2, 200th, Li–LFP	1 M LiPF$_6$ in EC/DMC/DEC (v/v/v = 1:1:1)	∼0.6	∼200 nm	[117]
C	Nafion + LiCl	Cast-coating Dip-casting	98.1% CE @1 mA/cm^2, 250th, ∼96% CE @ 3 mA/cm^2, 110th, Li–Cu Stable cycling for 1000 h @1 mA/cm^2, Li–Li ∼140 mAh/g @∼0.84 mA/cm^2, 150th, Li–LFP	1 M LiTFSI in DOL/DME (v/v = 1:1) 1 M LiTFSI in DOL/DME (v/v = 1:1) 1 M LiPF$_6$ in EC/DEC (v/v = 1:1)	1; 1 1 1.68	2.5 μm	[111]
C	Nafion + LLZTO	Blade-coating	98.5% CE @0.5 mA/cm^2, 350th; 97.7% CE@1.0 mA/cm^2, 150th Li–Cu 87.4% CR @1.0 mA/cm^2, 150th, Li–LFP	1 M LiTFSI in DOL/DME (v/v = 1:1) 1 M LiPF$_6$ in EC/DEC (v/v = 1:1)	0.5; 1.0 1.0	∼5 μm	[29]
C	DSN	Spin-coating Spin-coating Dip-coating	∼97.3% CE @0.25 mA/cm^2, 400th, Li–Cu ∼96.5% CE @0.5 mA/cm^2, 400th, Li–Cu Stable cycling for 2000 h @1 mA/cm^2; Li–Li ∼85% CR @0.5C, 160th, Li–NMC 532	1 M LiPF$_6$ in EC/DEC (v/v = 1:1)	0.5 1 1 2	\	[104]

ARTICLE IN PRESS

RESEARCH

TABLE 1 (CONTINUED)

Categories	Materials	Strategies	Electrochemical performance	Electrolytes	Areal capacity (mAh/cm²)	Thickness	Ref.
M[d]	Kimwipe paper	\	Stable cycling for 1000 h @2 mA/cm²; 1000 h @5 mA/cm²; 400 h @10 mA/cm², Li–Li	1.85 M LiCF₃SO₃[q] in DOL/DME (v/v = 1:1)	6	\	[121]
M	Nafion + PVDF	Cast-coating	Stable cycling for 200 h @1.1 mA/cm², Li–Li / Stable cycling for 100 cycles @1.17 mA/cm², Li–S	1 M LiTFSI in DOL/DME (v/v = 1:1) / 1 M LiTFSI in DOL/DME (v/v = 1:1)	1.1 / 1.17	3 μm	[122]
M	TSP	Blade-coating	Stable cycling for 500 h @1 mA/cm²; 300 h @2 mA/cm²; 400 h @10 mA/cm²; ~70 h @5 mA/cm², Li@TSP-Cu‖Li / 98.14% (Avg.) CE @1 mA/cm², >100 cycles, Li–Cu / 616.8 mAh/g @ 0.369 mA/cm², 150th, Li@TSP-Cu‖S	0.5 M LiCF₃SO₃ and 0.5 M LiNO₃ in DOL/DME (v/v = 1:1)	1; 1; 2 / 1 / 1.84	~800 nm	[100]
M	Agarose (AG)	\	98.5% CE@\ mA/cm², 100th, Li–Cu / Stable cycling for 650 h @0.5 mA/cm², 550 h @1 mA/cm²; 250 h @2 mA/cm², Li@AG-Cu‖Li / 102 mAh/g @1.2 mA/cm², 500th, Li @AG-Cu‖LFP	0.5 M LiCF₃SO₃ and 0.5 M LiNO₃ in DOL/DME (v/v = 1:1) / 0.5 M LiCF₃SO₃ and 0.5 M LiNO₃ in DOL/DME (v/v = 1:1) / 1 M LiPF₆ in EC/DMC/EMC (v/v/v = 1:1:1)	1 / 1 / 0.3	1 μm	[120]

a: polymers with nonpolar groups; b: polymers with polar groups; c: polymers with charged groups; d: polymers with multi-type of ionic conductive groups; e: grafted polymer skin: poly((N-2,2-dimethyl-1,3-dioxolane-4-methyl)-5-norbornene-exo-2,3-dicarboximide); f: capacity retention; g: ethylene carbonate; h: ethyl methyl carbonate; i: fluoroethylene carbonate; j: dimethyl carbonate; k: tetraethylene glycol dimethyl ether; l: dimethyl carbonate; m: graphene–polydopamine + PEO composite layer; n: diethylene glycol dimethyl ether; o: (poly (ethylene glycol) dimethacrylate); p: electrochemical reduction; q: lithium trifluoromethanesulfonate salt

Most of the polymers with multi-type ionic conductive groups applied in this area are natural or natural-derived materials. With the renewable source, facile and environmental-friendly fabrication process, more research attentions should be paid to this type of polymeric materials as the artificial SEI films toward the target of sustainable future. Compositing of the polymeric materials with inorganic filler such as Al_2O_3, TiO_2 to enhance the mechanical strength and ionic conductivity or co-grafted with other polymers to improve the viscoelasticity and binding ability should also be useful strategies to improve their electrochemical performance as artificial SEI film.

Conclusions and perspectives
Conclusions
In this review, we have summarized the recent progress on ionic conductive polymers as artificial SEI films for Li metal electrode, and the fundamental design principles in constructing an efficient artificial SEI protecting layer was discussed during this process. Rational design of polymeric artificial SEI films that can induce controllable Li⁺ deposition, suppress dendritic Li growth, and accommodate the huge volume variations is a highly promising approach to promote the practical applications of LMBs. An ideal artificial SEI should features with high ionic conductivity, mechanical robustness, high electrochemical stability. The ionic conductive polymers used as artificial SEI films can be divided into four categories: polymers with nonpolar groups, polar groups, charged groups and multi-type of ionic conductive groups. Polymers with different types of ionic conductive groups have their own advantages and disadvantages as artificial SEI films. For polymers with non-polar groups, mostly PEO-based polymers, have a high dielectric constant, a large electron donor number for Li⁺ and high chain flexibility, which allows efficient Li⁺ transport [64,125]. Moreover, the mature experience gained from the previous studies as solid/gel electrolyte can also provide some guidance for designing polymeric artificial SEI films in LMBs. However, the ionic conductivities of these polymers are inversely related to their degree of crystallinity, which is considered to be detrimental to charge transport owing to the slower polymer chain dynamics under crystal state [126,127]. For ionic conducting polymers with polar groups, due to the dipole–dipole interaction between electrolyte solvent and polar groups of artificial SEI film, the reactivity of free carbonate solvents are greatly suppressed, which facilitates the formation of SEI layer with more salt anions (e.g., PF^{6-} or TFSI⁻) [128]. With more inorganic components, the formed SEI layer can suppress the side reactions between the organic electrolyte and Li metal in a more efficient manner, while these dipole–dipole interactions may vary with different polar groups and electrolyte systems (e.g., ether system in Li–S battery). The ionic conducting polymers with charged groups can effectively improve the cationic transference number, i.e., t_{Li^+}, achieving a homogeneous Li⁺ plating/stripping behavior and suppressed Li–dendrite growth [29]. Nevertheless, some polymers with charged groups, such as Nafion, have poor mechanical properties, and incorporation of inorganic filler is a viable approach achieving improved electrochemical performance. Polymers with multi-type ionic conductive groups possess the attributes of each conductive groups, while the

15

RESEARCH
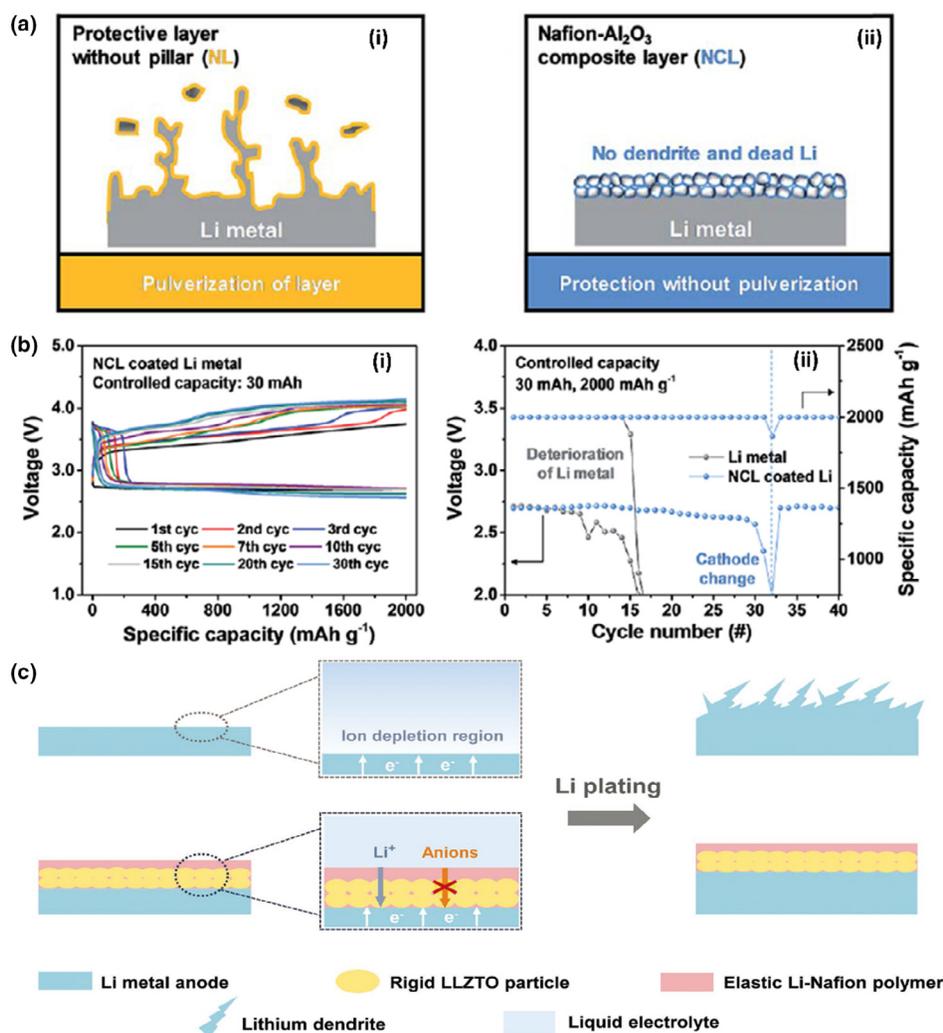
FIGURE 10

(a) Schematic illustrations of side reactions on the Li metal anodes with Nafion layer (NL, i) and composite Nafion layer (CPL, ii). (b) Electrochemical performance of Li–O$_2$ pouch cells: (i) galvanostatic charge/discharge voltage profiles with artificial SEI-coated Li as anode. (ii) Cycling performance with bare Li and artificial SEI-coated Li as anode. Reproduced with permission [65]. Copyright 2019. The Royal Society of Chemistry. (c) Li$^+$ deposition process with and without dual-layer artificial SEI layer. Reproduced with permission [29]. Copyright 2019. WILEY-VCH Verlag GmbH & Co. KGaA, Weinheim.

fabricating process may be more complicated. Biomass-derived polymeric materials are the main focus for this type of artificial SEI films, which will benefit the sustainable development while their long-term electrochemical stability may be a potential issue. Rational design of polymeric materials with high interactions (binding ability) with Li$^+$ and Li metal will significantly suppress the dendritic Li growth and side reaction between the electrolyte and Li metal.

Many efforts have been devoted to artificial SEI films containing the ceramic electrolyte because the ceramic electrolyte will not only provide sufficient Li$^+$ transfer channels but also improve the mechanical robustness that can mitigate the growth of Li dendrites. Constructing hybrid films by compositing ionic conducting polymers with other inorganic materials, such as the TiO$_2$, Al$_2$O$_3$ and LiCl can also improve the ionic conductivity and mechanical strength of the aforementioned artificial SEI films, achieving improved electrochemical performance due to the synergistic effect of both components.

Perspectives

The chemical components of actual artificial SEI is complicated and highly depended on the interfacial reactions between the Li–metal and electrolyte. Besides, the paired cathode materials with different operating voltages and active species will also play an important role in constructing the artificial SEI films on the Li metal surface. Although huge achievements have been obtained in constructing artificial SEI films for Li–metal electrode with improved the electrochemical performance, the feasibility and reliability of artificial SEI films still need further studies towards the target of LMBs with long cycle life and high energy density.

Based on the fundamental principles of constructing polymeric artificial SEI films, the following research topics are highly promising in this field: (1) Safety is always the most important requirement for the rechargeable batteries. With the development of the LMBs, batteries with higher energy density presented new challenges for the artificial SEI films, and polymers
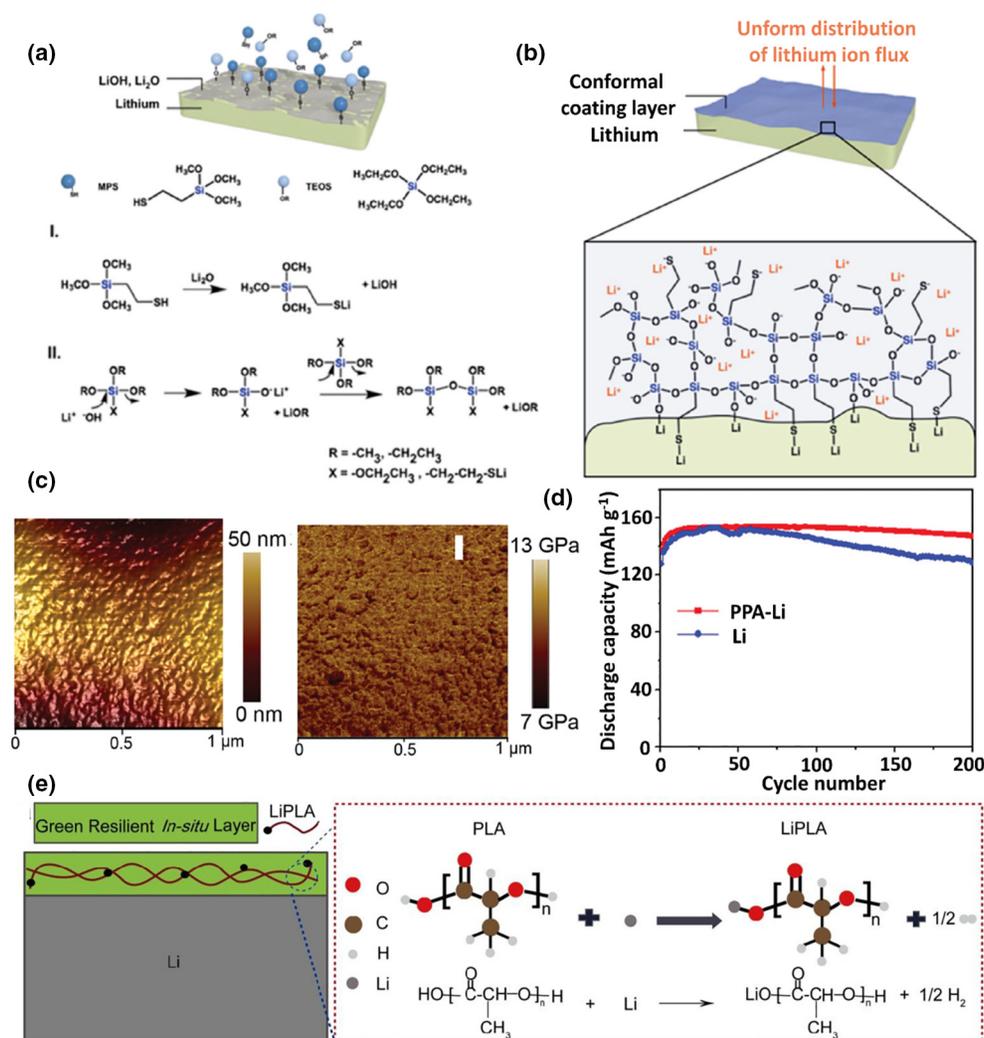
FIGURE 11

(a) Illustration of forming hermetic coatings of hybrid silicate on Li metal surface. (b) Formation of the artificial SEI layer on the Li metal surface. Reproduced with permission [116]. Copyright 2017. WILEY-VCH Verlag GmbH & Co. KGaA, Weinheim. (c) AFM images of PPA–Li coated Li anode (left) and corresponding Young's modulus mapping (right). (d) Cycling performance of Li–LFP cells with bare and PPA–Li coated Li as anodes. Reproduced with permission [117]. Copyright 2015. WILEY-VCH Verlag GmbH & Co. KGaA, Weinheim. (e) Schematic illustration of the in situ synthesis of LiPLA based artificial SEI film. Reproduced with permission [118]. Copyright 2019. American Chemical Society.

with higher electrochemical and thermal stability are highly recommended. (2) Quantitative description of the impacting factors is meaningful for constructing artificial SEI film with optimal battery performance. The polymeric artificial SEI film should feature with good ionic conductivity, high Young's modulus, appropriate thickness and high chemical/electrochemical stability. Taking solid electrolyte as an example, the simulation demonstrated that decent modulus (10–100 MPa) combined with immobilization of a fraction of anions (10%) can also efficiently resist the growth of Li dendrites [129]. Similarly, as shown in Table 1, protecting layers with different film thickness were utilized in different reports, which is related to the physicochemical properties of the polymers and the current density (or area capacity) utilized in electrochemical test. Moreover, the suitable thickness should be in an interval instead of a certain value, while in some reports, the relationship between the film thickness and the electrochemical performance have not been care-

fully studied. To better understand the interactions between the polymeric artificial SEI film, electrolyte and intrinsic SEI layer, quantitative description of the film thickness is required, which should provide useful guidance for rational design high-performance polymeric artificial SEI films. Moreover, the electrolyte uptake and ionic conductivity of polymeric films under the swollen state should also be considered due to the fact that their ionic conductivities are also highly dependent on the swelling capability. (3) Higher energy density and longer lifespan of assembled batteries to evaluate the constructed artificial SEI films. The rechargeable batteries with areal capacity of higher than $2 \, \text{mAh cm}^{-2}$ (or $3 \, \text{mAh cm}^{-2}$) are necessary towards the practical applications. In the aspect of lifespan, according to the national standard of China (GB/T 31484–2015), the capacity retention of power batteries should be higher than 90% after 500 cycles or 80% after 1000 cycles at the current density of 1C based on the initial cycle. (4) Establish a standard to evaluating the per-
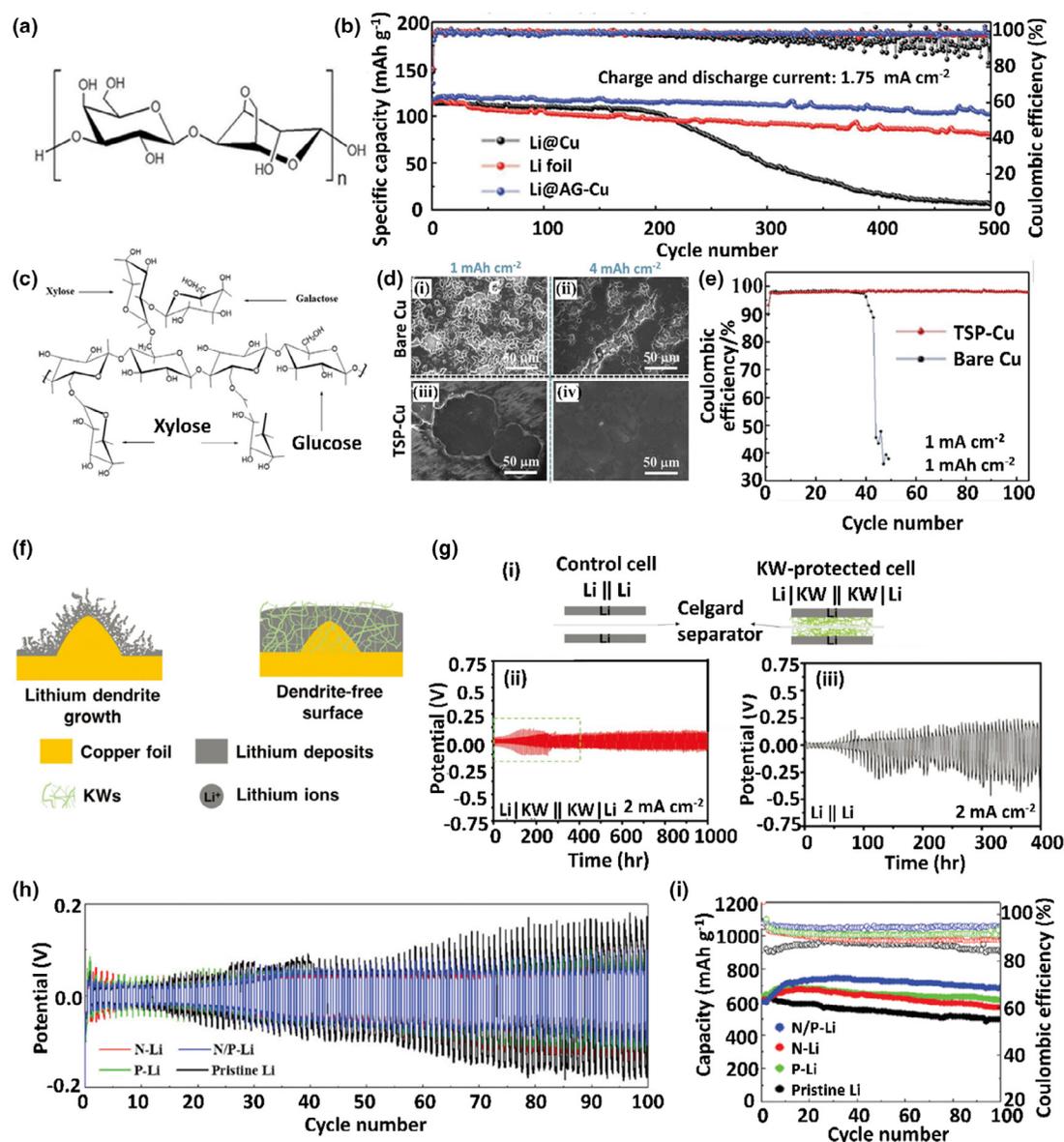
FIGURE 12

(a) Chemical structure of the agarose (AG). (b) Cycling performance of Li–LFP cells with Li@Cu, bare Li and Li@AG-Cu as anodes. Reproduced with permission [120]. Copyright 2018, WILEY-VCH Verlag GmbH & Co. KGaA, Weinheim; (c) Chemical structure of tamarind seed polysaccharide. (d) SEM images of Li deposits on the bare Cu foil (i, ii) and the polysaccharide coated Cu substrate (iii, iv). (e) CEs of TSP modified and bare Cu electrodes at a current density of 1 mA cm^{-2}. Reproduced with permission [100]. Copyright 2019, Elsevier. (f) Illustrations of Li$^+$ deposition with (right) and without (left) Kimwipe paper. (g) (i) The configurations of Li–Li symmetric cells with and without protected Kimwipe paper. (ii) and (iii) are the voltage versus time profiles at 2 mA cm^{-2} with and without Kimwipe paper, respectively. Reproduced with permission [121]. Copyright 2017, WILEY-VCH Verlag GmbH & Co. KGaA, Weinheim. (h) Electrochemical performance of Li–Li symmetric cells consisting of pristine Li, Nafion-coated Li (N-Li), PVDF-coated Li (P-Li) and Nafion/PVDF-coated Li (N/F-Li). (i) Cycling performance of Li–S cells with different Li anodes. Reproduced with permission [122]. Copyright 2017. The Royal Society of Chemistry.

formance of artificial SEI films, which will allow the community to cross-compare different systems. For example, artificial SEI film with thickness of 1 μm on Cu foil along with the reported CEs of the first few cycles at current density of 0.5 mA cm^{-2} and plating capacity of 1 mAh cm^{-2} may be set as a standard for Li–Cu cell. (5) Studies based on multidisciplinary fields — polymer physics, polymer chemistry, nanotechnology, interface and so on are highly recommended for broader approach investigation. For example, widely applied in the field of catalysis, MOFs and COFs with abundant porous structures and mechanical robustness may also be promising as high performance artificial SEI [130]. (6) Utilization of bio-derived materials as artificial SEI of Li–metal electrode towards the target of sustainable future is also important.

With great promise to overcome the bottleneck of energy density in current LIBs, LMBs have been attracting increased research attentions. Rational design of polymeric artificial SEI for Li–metal anode has been demonstrated a viable approach to the target of achieving LMBs with a high energy density, high safety and long cycling lifetime, while further studies in this area and other related studies like solid-state electrolyte, cathode and electrolyte–cathode interface are still highly demanded.

Declaration of Competing Interest

Acknowledgements

References

[1] Y. Zhao et al., Adv. Mater. 31 (12) (2019) 1806532.
[2] P. Albertus et al., Nat. Energy 3 (1) (2018) 16–21.
[3] N. Nitta et al., Mater. Today 18 (5) (2015) 252–264.
[4] H. Zhao et al., Nano Lett. 15 (12) (2015) 7927–7932.
[5] Y. Wang et al., Nano Energy 39 (2017) 200–210.
[6] S. Gao et al., Nano Energy 73 (2020) 104804.
[7] Y. Pan et al., Chem. Eur. J. 25 (2019) 10976–10994.
[8] M. Wan et al., Nat. Commun. 11 (1) (2020) 829.
[9] X.-B. Cheng et al., Chem. Rev. 117 (15) (2017) 10403–10473.
[10] P.G. Bruce et al., Nat. Mater. 11 (1) (2012) 19–29.
[11] Y. Wang et al., Carbon 132 (2018) 420–429.
[12] Q. Huang et al., Nat. Commun. 10 (1) (2019) 5586.
[13] B. Zhu et al., Chem. Sci. 10 (30) (2019) 7132–7148.
[14] Y. Pan et al., ACS Appl. Energy Mater. 3 (4) (2020) 3387–3396.
[15] S. Gao et al., Electrochim. Acta 327 (2019) 135058.
[16] R. Zhang et al., Adv. Sci. 4 (3) (2017) 1600445.
[17] Ma et al., Nano Lett. 19 (2) (2019) 1387–1394.
[18] X.-Q. Zhang et al., Adv. Mater. Interfaces 5 (2) (2018) 1701097.
[19] G. Zheng et al., Nat. Nanotechnol. 9 (8) (2014) 618–623.
[20] X. Xu et al., J. Energy Chem. 27 (2) (2018) 513–527.
[21] R. Xu et al., Adv. Funct. Mater. 28 (8) (2018) 1705838.
[22] C. Zhang et al., J. Electrochem. Soc. 166 (15) (2019) A3675–A3678.
[23] Y. Liu et al., Energy Storage Mater. 25 (2020) 131–136.
[24] C. Yang et al., Adv. Mater. 29 (36) (2017) 1701169.
[25] G.H. Moon et al., Chem. Comm. 55 (2019) 6313–6316.
[26] M. Ling et al., Nano Energy 38 (2017) 82–90.
[27] N. Akhtar et al., Electrochim. Acta 282 (2018) 758–766.
[28] J.-M. Tarascon et al., Nature 414 (2001) 359–367.
[29] R. Xu et al., Adv. Mater. 31 (19) (2019) 1808392.
[30] H. Wang et al., Chem 5 (2) (2019) 313–338.
[31] W. Xu et al., Energy Environ. Sci. 7 (2) (2014) 513–537.
[32] L. Li et al., Chem. Commun. 54 (50) (2018) 6648–6661.
[33] Y. Zhang et al., Mater. Today 33 (2020) 56–74.
[34] Y. Wang et al., J. Mater. Sci. 54 (5) (2019) 3671–3693.
[35] Y. Feng et al., J. Mater. Chem. A 7 (11) (2019) 6090–6098.
[36] B. Zhu et al., Adv. Mater. 29 (2) (2017) 1603755.
[37] J. Yamaki et al., J. Power Sources 74 (2) (1998) 219–227.
[38] C. Fringant et al., Electrochim. Acta 40 (4) (1995) 513–523.
[39] H. Liu et al., EnergyChem 1 (1) (2019) 100003.
[40] G. Yasin et al., Energy Storage Mater. 25 (2020) 644–678.
[41] D. Lin et al., Nat. Nanotechnol. 12 (3) (2017) 194–206.
[42] S.F. Liu et al., J. Alloy. Compd. 730 (5) (2018) 135–149.
[43] Y. Liu et al., Chem. Eng. J. 371 (1) (2019) 294–300.
[44] X. Cui et al., ACS Sustainable Chem. Eng. 6 (8) (2018) 11097–11104.
[45] Y. Kim et al., ACS Nano 12 (5) (2018) 4419–4430.
[46] M.-H. Ryou et al., Adv. Funct. Mater. 25 (6) (2015) 834–841.
[47] Y. Feng et al., Energy Storage Mater. 25 (2020) 172–179.
[48] P. Shi et al., Adv. Mater. 31 (37) (2019) 1902785.
[49] K. Yan et al., Angew. Chem. Int. Ed. 58 (33) (2019) 11364–11368.
[50] B. Song et al., ACS Energy Lett. 4 (10) (2019) 2402–2408.
[51] E. Peled et al., J. Electrochem. Soc. 164 (7) (2017) A1703–A1719.
[52] P. Yao et al., Mater. Chem. Front. 3 (2) (2019) 339–343.
[53] Q. Lu et al., Adv. Mater. 29 (13) (2017) 1604460.
[54] L. Matkovska et al., Nanoscale Res. Lett. 12 (2017) 423.
[55] W. Luo et al., Nano Lett. 15 (9) (2015) 6149–6154.
[56] W. Choi et al., Sci. Rep. 7 (1) (2017) 12037.
[57] J. Liang et al., Angew. Chem. Int. Ed. 59 (16) (2020) 6561–6566.
[58] S. Xu et al., Nano Lett. 18 (6) (2018) 3926–3933.
[59] R. Tian et al., ChemSusChem 11 (18) (2018) 3243–3252.
[60] P. Li et al., Angew. Chem. Int. Ed. 58 (7) (2019) 2093–2097.
[61] K. Chen et al., Energy Storage Mater. 18 (2019) 389–396.
[62] Y. Yuan et al., J. Energy Chem. 37 (2019) 197–203.
[63] H. Chen et al., Adv. Energy Mater. 9 (22) (2019) 1900858.
[64] A.A. Assegie et al., Nanoscale 10 (13) (2018) 6125–6138.
[65] W.-J. Kwak et al., J. Mater. Chem. A 7 (8) (2019) 3857–3862.
[66] J. Luo et al., Adv. Energy Mater. 8 (2) (2018) 1701482.
[67] P.-F. Cao et al., Adv. Funct. Mater. 28 (22) (2018) 1800741.
[68] P.-F. Cao et al., Macromolecules 53 (9) (2020) 3591–3601.
[69] R. Xu et al., Matter 1 (2) (2019) 317–344.
[70] L. Qi et al., Chem. Eur. J. 26 (19) (2020) 4193–4203.
[71] L. Jiao et al., Energy Storage Mater. 23 (2019) 112–136.
[72] J. Lopez et al., Nat. Rev. Mater. 4 (5) (2019) 312–330.
[73] C. Liebenow et al., J. Appl. Electrochem. 26 (7) (1996) 689–692.
[74] Y.M. Lee et al., J. Power Sources 119–121 (1) (2003) 964–972.
[75] J. Lopez et al., J. Am. Chem. Soc. 140 (37) (2018) 11735–11744.
[76] X. Yu et al., ACS Appl. Mater. Interfaces 7 (29) (2015) 15961–15967.
[77] W. Zhou et al., Adv. Mater. 31 (4) (2019) 1805574.
[78] T.N.T. Phan et al., Polym. Int. 68 (1) (2019) 7–13.
[79] J. Zhu et al., Prog. Polym. Sci. 90 (2019) 118–163.
[80] X. Judez et al., J. Electrochem. Soc. 165 (1) (2017) A6008–A6016.
[81] Y. Yao et al., Energy Environ. Sci. 5 (7) (2012) 7927–7930.
[82] M. Vosgueritchian et al., Adv. Funct. Mater. 22 (2) (2012) 421–428.
[83] D. Shao et al., ChemElectroChem 1 (10) (2014) 1679–1687.
[84] L. Yan et al., Sustainable Energy Fuels 2 (7) (2018) 1574–1581.
[85] H. Chen et al., Sci. Rep. 3 (2013) 1910.
[86] I.S. Kang et al., J. Electrochem. Soc. 161 (1) (2013) A53–A57.
[87] G. Ma et al., J. Mater. Chem. A 2 (45) (2014) 19355–19359.
[88] Y. Zhang et al., Sci. Bull. 64 (13) (2019) 910–917.
[89] J.-H. Kim et al., ACS Appl. Mater. Interfaces 8 (47) (2016) 32300–32306.
[90] D.J. Lee et al., Adv. Mater. 28 (5) (2016) 857–863.
[91] W.-J. Kwak et al., Adv. Energy Mater. 8 (9) (2018) 1702258.
[92] C. Yang et al., Nano Res. 10 (12) (2017) 4256–4265.
[93] C. Zhang et al., Electrochim. Acta 306 (20) (2019) 407–419.
[94] L. Chen et al., ACS Appl. Mater. Interfaces 10 (8) (2018) 7043–7051.
[95] H. Dong et al., J. Power Sources 423 (31) (2019) 72–79.
[96] A.C. Kozen et al., Chem. Mater. 29 (15) (2017) 6298–6307.
[97] Y. Gao et al., J. Am. Chem. Soc. 139 (43) (2017) 15288–15291.
[98] Y. Sun et al., Adv. Mater. 31 (4) (2019) 1806541.
[99] X. Wang et al., ACS Appl. Mater. Interfaces 11 (5) (2019) 5159–5167.
[100] J.-H. You et al., Electrochim. Acta 299 (10) (2019) 636–644.
[101] Z. Hu et al., Chem. Mater. 29 (11) (2017) 4682–4689.
[102] I.C. Jang et al., J. Electrochem. Soc. 161 (5) (2014) A821–A826.
[103] H. Lee et al., J. Power Sources 284 (15) (2015) 103–108.
[104] Z. Yu et al., Joule 3 (11) (2019) 2761–2776.
[105] X. Li et al., J. Mater. Chem. A 5 (40) (2017) 21362–21369.
[106] Y. Wang et al., ACS Appl. Mater. Interfaces 11 (5) (2019) 5168–5175.
[107] J. Song et al., Sci. Rep. 5 (2015) 14458.
[108] P.-F. Cao et al., Polymer 124 (25) (2017) 117–127.
[109] P.-F. Cao et al., ACS Appl. Mater. Interfaces 10 (4) (2018) 3470–3478.
[110] N.-W. Li et al., Angew. Chem. Int. Ed. 57 (6) (2018) 1505–1509.
[111] S. Li et al., Energy Storage Mater. 18 (2019) 205–212.
[112] C. Shen et al., Nano Energy 19 (2016) 68–77.
[113] T.-Z. Zhuang et al., Small 12 (3) (2016) 381–389.
[114] Y. Cao et al., PCCP 13 (17) (2011) 7660–7665.
[115] S. Jiang et al., Chem. Asian J. 13 (10) (2018) 1379–1385.
[116] F. Liu et al., Adv. Energy Mater. 8 (6) (2018) 1701744.
[117] N.-W. Li et al., Adv. Mater. 28 (9) (2016) 1853–1858.
[118] N. Wu et al., ACS Appl. Mater. Interfaces 11 (46) (2019) 43200–43205.
[119] W. Wang et al., Electrochim. Acta 56 (21) (2011) 7347–7351.
[120] S.-J. Zhang et al., Small 14 (31) (2018) 1801054.
[121] C.-H. Chang et al., Adv. Sustainable Syst. 1 (1-2) (2017) 1600034.
[122] J. Luo et al., Chem. Commun. 53 (5) (2017) 963–966.
[123] S. Kim et al., Electrochim. Acta 282 (20) (2018) 343–350.
[124] D.J. Lee et al., Electrochem. Commun. 40 (2014) 45–48.
[125] J. Zhang et al., Nano Lett. 15 (5) (2015) 3398–3402.
[126] R. Khurana et al., J. Am. Chem. Soc. 136 (20) (2014) 7395–7402.

[127] Z. Xue et al., J. Mater. Chem. A 3 (38) (2015) 19218–19253.
[128] J. Bae et al., Energy Environ. Sci. 12 (11) (2019) 3319–3327.
[129] M.D. Tikekar et al., Sci. Adv. 2 (7) (2016) 1600320.
[130] T. Kitao et al., Chem. Soc. Rev. 46 (11) (2017) 3108–3133.

RESEARCH